Review of Palaeobotany and Palynology 299 (2022) 104604

Contents lists available at ScienceDirect

Review of Palaeobotany and Palynology

journal homepage: www.elsevier.com/locate/revpalbo

Microspores, megaspores, palynofacies, and depositional history of the upper Givetian Maywood Formation, Northern Wyoming, USA

Mercedes Di Pasquo [a,*], Mingxi Hu [b], Michał Zatoń [c], Paul Myrow [b]

[a] Laboratory of Palynostratigraphy and Paleobotany, Centro de Investigación Científica y de transferencia de tecnología a la producción (CONICET-ER-UADER), Diamante CP [E3105BWA], Entre Ríos, Argentina
[b] Department of Geology, Colorado College, Colorado Springs, CO 80903, USA
[c] Institute of Earth Sciences, University of Silesia in Katowice, Będzińska 60, 41-200 Sosnowiec, Poland

ARTICLE INFO

Article history:
Received 30 November 2021
Received in revised form 6 January 2022
Accepted 9 January 2022
Available online 13 January 2022

Keywords:
Palynoflora
Middle Devonian
Taghanic crisis
Paleoenvironments
Paleoecology

ABSTRACT

Incised valley-fill deposits of the Middle Devonian Maywood Formation at Cottonwood Canyon, Wyoming, USA, contains a significant palynological record. Twenty-six palynotaxa were recovered, of which 21 species have wide paleogeographical distribution. The presence of the microspores *Samarisporites triangulatus* and *Contagisporites optivus*, as well as other Givetian index taxa, points to a late Givetian age (*C. optivus*/*S. triangulatus* palynozone) of the Maywood Formation. The palynoflora investigated may be correlative with the *hermanni* conodont Zone or a younger zone, and thus they record the latest Taghanic crisis or the earliest post-Taghanic interval. The playnoflora includes progymnosperms that had a tree-like habit (Aneurophytales and Archaeopteridales) characteristic of proximal fluvio-lacustrine settings of floodplains and paralic environments of internal basins. Spores of the herbaceous lycopsid Selaginellales, shrubby lycopods Protolepidodendrales, and primitive ferns, indicate a proximity of terrestrial plant habitats near the Maywood paleovalley. Additionally, the palynofacies (1) have amorphous organic matter and few algal remains of marine origin (*Quadrisporites*, *Dictyotidium*), (2) exist in association with assemblages of monospecific microconchid tubeworms that may have colonized non-biomineralized algae, and (3) are in strata that lack other benthic fossils, all of which indicate that the Maywood paleovalley record fluctuations of salinity. These were generated by mixing of marine and freshwater inputs within the estuarine channel, which was developed along the paleoshorelines of the Maywood Sea.

1. Introduction

The Devonian Maywood Formation records deposition within estuarine paleovalleys that were incised into the Lower Devonian Beartooth Butte Formation and Upper Ordovician bedrock of the Bighorn Formation (Sandberg and McMannis, 1964). The Beartooth Butte deposits also fill paleovalleys, and both these and the Maywood paleovalleys were formed prior to the Late Devonian Antler Orogeny (Johnson and Pendergast, 1981; Dorobek et al., 1991; Ketner, 2012), suggesting that their erosion and subsequent filling were driven by eustasy (Johnson et al., 1985; Johnson and Sandberg, 1989). A Givetian age was assigned to the Maywood Formation at Cottonwood Canyon based on previous a preliminary analysis of its palynological assemblages (Zatoń et al., 2021).

Episodic early to middle Devonian transgressive–regressive cycles of western Laurentia have been recognized, and these were responsible for the erosion and infilling of channels cut into bedrock across the western U.S. (Sandberg and McMannis, 1964; Johnson and Sandberg, 1989; Grader and Dehler, 1999). Globally, Devonian high frequency, eustatic sea-level changes correlate to a series of short-term shifts in marine oxygenation, climate conditions, and fauna/floral evolutions (Algeo et al., 2001; Goddéris and Joachimski, 2004; Buggisch and Joachimski, 2006; van Geldern et al., 2006; Aboussalam and Becker, 2011). The Givetian in particular records: 1) the narrowing of the Rheic ocean between Laurussia–Baltica and Gondwana (Nance et al., 2012; Streel et al., 2021); 2) a warming pulse in the long-term climatic cooling of the Devonian (Joachimski et al., 2004; van Geldern et al., 2006; Brugger et al., 2019); 3) increased cosmopolitanism and spread of both marine (Young, 2003; Lukševičs et al., 2010; Aboussalam and Becker, 2011; Young and Lu, 2020) and terrestrial species (Xue et al., 2018; Wan et al., 2019); and 4) the evolution and diversification of terrestrial flora (Gutak et al., 2011; Cornet et al., 2012; Shen et al., 2020). By this time, vascular plants had developed secondary supporting tissues and extractive root systems that allowed them to increase in size and biomass (Algeo and Scheckler, 1998), and forests first appeared in the

* Corresponding author.
E-mail addresses: medipa@cicyttp.org.ar (M. Di Pasquo), m_hu@coloradocollege.edu (M. Hu), mzaton@wnoz.us.edu.pl (M. Zatoń), pmyrow@coloradocollege.edu (P. Myrow).

https://doi.org/10.1016/j.revpalbo.2022.104604
0034-6667/

Givetian (Stein et al., 2020; Davies et al., 2021). Moreover, there was a turnover of early plant clades, such as trimerophytes and zosterophyllophytes to euphyllophytes (Steemans et al., 2012; Xue et al., 2018; Wan et al., 2019; Qie et al., 2019), and a transition from aneurophytes to archaeopterids (Turnau, 2014; Wan et al., 2019; Shen et al., 2020).

This study presents a detailed palynologic analysis of the Maywood Formation exposed at Cottonwood Canyon, Wyoming (Fig. 1), which provides insights into the paleoenvironmental conditions of these remarkable channel-fill deposits, reveals the nature of the floral communities, and allows for regional and global correlations of these strata.

2. Geology and paleontology of the Maywood Formation

The channel-fill deposits of the Maywood Formation (Sandberg, 1961b; Sandberg and McMannis, 1964) are correlative with the Souris River Formation of the Williston Basin (Sandberg, 1963) and the lower part of Beaverhill Lake Formation of Alberta Basin, Canada (Kauffman

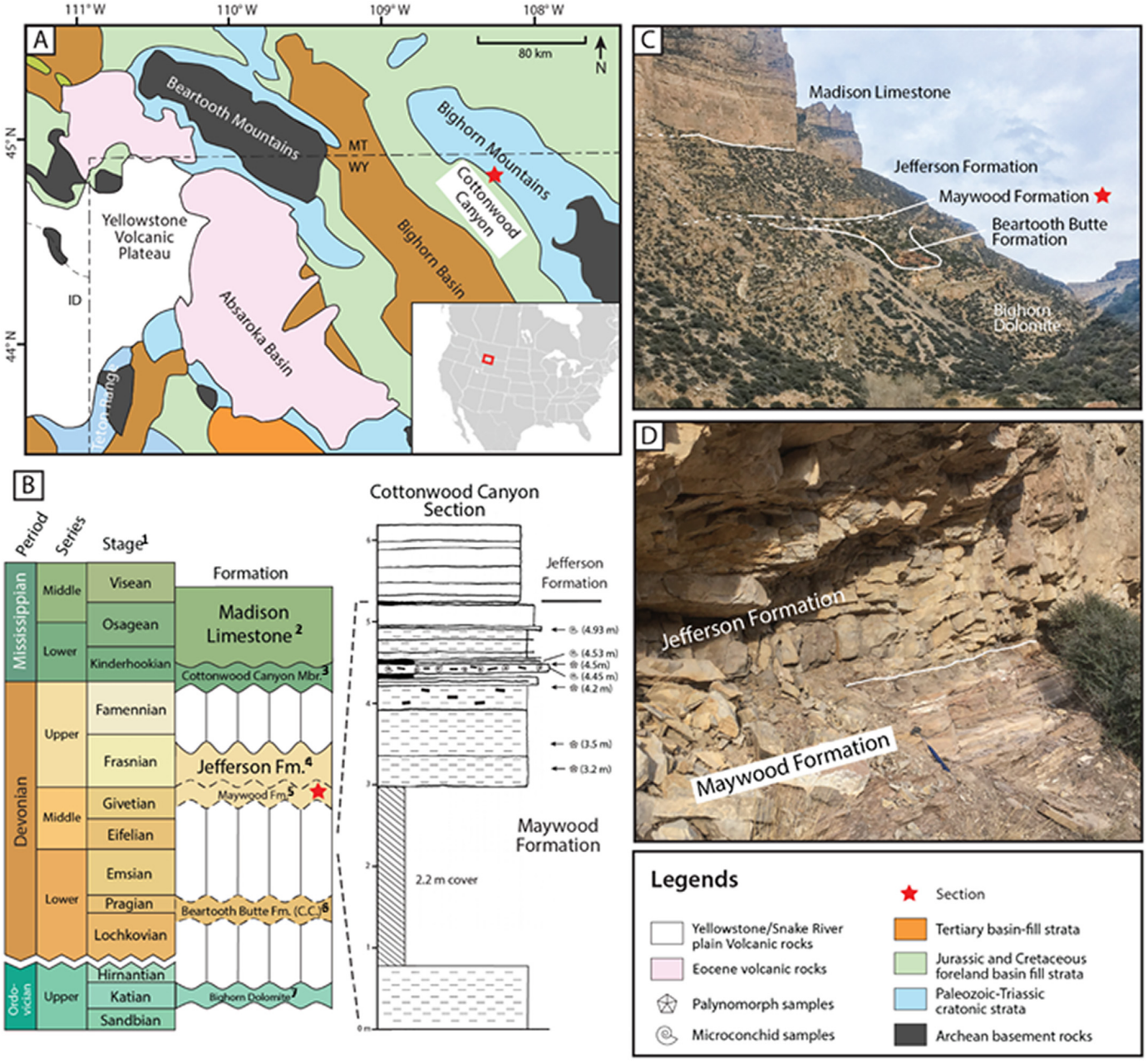

Fig. 1. A. Generalized geologic map of northern Wyoming (USA) showing the study site at Cottonwood Canyon (red star) in Bighorn Mountains (adapted from Malone et al., 2017). **B.** Devonian and Mississippian chronostratigraphic framework from Cohen et al. (2020), and stratigraphic units in Wyoming, in which vertical lines and wavy horizontal lines represent depositional hiatuses between formations. The Maywood Formation at Cottonwood Canyon directly overlies the Bighorn Dolomite and underlies the Jefferson Formation with a sharply gradational or slightly disconformable contact. The Maywood Formation measured section includes stratigraphic height (in meters) and black rectangles representing large pieces of coal fragments and plant debris. Numbers in brackets indicate stratigraphic position of microconchid and palynologic samples. **C.** General view of the Devonian and Carboniferous succession at Cottonwood Canyon in the Bighorn Mountains. **D.** Maywood and Jefferson formations at Cottonwood Canyon, showing the red, fine-grained strata of the upper Maywood Formation and contact with the thin to medium bedded dolomudstone of the basal Jefferson Formation. Superscripts in Fig. B: 1 = North American stages Kinderhookian and Osagean are used for Lower Mississippian stages instead of Tournaisian; 2 = Peterson (1981); 3 = Sandberg (1967); 4 = Sandberg (1963); 5 = Sandberg (1963); 6 = Beartooth Butte = Cottonwood Canyon (C.C.), Wyoming; 7 = Holland and Patzkowsky (2009). (For interpretation of the references to color in this figure legend, the reader is referred to the web version of this article.)

and Earll, 1963). Sandberg and McMannis (1964) suggested that the Maywood might be conformably overlain by the Jefferson Formation (Fig. 1B–D), based on a gradational, albeit sharply gradational, lithologic transition. $\delta^{13}C$ (bulk) isotope data indicate a negative shift of ~2.5‰ across the Maywood–Jefferson formation contact, suggesting a possible minor disconformity at this level (Myrow and Hu, unpublished data).

The Maywood Formation is regionally highly variable in thickness, ranging from <5 m to >100 m at its type locality in Montana (Sandberg, 1961a). At the Cottonwood Canyon site, the Maywood has a poorly exposed, 80 cm thick, massive weathering basal unit of yellow to tan dolosiltite with fish fossil fragments, an overlying 2.2 m thick covered interval, and then 2.24 m of calcisiltite/dolosiltite, grainstone, and shale (Zatoń et al., 2021; Fig. 1C–D). The recessively weathered calcisiltite/dolosiltite is dark brown to black, and locally highly carbonaceous with macerated plant remains and stem impressions. It also contains a few scattered microconchids (~1 mm diameter on average), a type of tentaculitoid tubeworms with close affinities to such 'lophophorates' as bryozoans and brachiopods (Taylor and Vinn, 2006; Zatoń et al., 2021). A few thin (1–3 cm), recessive, carbonaceous, black to dark gray shale beds are present, and these weather tan to light-gray.

The silty facies of the Maywood is interbedded with mm-scale beds to 15 cm thick intervals dominated by fine to coarse grainstone. The grainstone consists almost entirely of coiled microconchids (avg. ~1 mm), with scattered phosphatic fish remains (Zatoń et al., 2021). The microconchids, represented by a single species *Aculeiconchus sandbergi*, consist of complete and fragmented tubes, which are generally oxidized, pyrite-coated, and densely packed (Zatoń et al., 2021). The grainstone contains oval-shaped, dispersed coal pebbles up to 3 cm across, in addition to carbonized macerated plant stems, and plant impressions. Beds of microconchid grainstone are present at 4.34 m, 4.53 m, and 4.93 m (Fig. 1B). Both microconchids (Caruso and Tomescu, 2012) and fish fossils (Sandberg, 1963; Elliot and Ilyes, 1996; Elliot and Johnson, 1997; Fiorillo, 2000) have been noted in a Beartooth Butte Formation (Fig. 1B) section in the south wall of Cottonwood Canyon ~1 km to the southeast of our field site. Our palynologic analysis of four samples (siltite and grainstone) from the Maywood has yielded well-preserved microspores and megaspores and subordinated algal remains (Fig. 2). Screening of the samples revealed megaspores that are both dispersed, and embedded with coiled microconchids, carbonaceous plant debris (Plates I–II), and scarce fish remains. The biostratigraphic and paleoenvironmental significance of these fossils are explored, based on diagnostic taxa and palynofacies features of palynoassemblages.

3. Location and methods

We examined the Maywood Formation at Cottonwood Canyon, directly east of Lovell, Wyoming (N44°52′14.0″; W108°03′26.5″). We measured a 5.24 m thick section of the Maywood along the edge of a wide channel fill where the formation rests directly on the Upper Ordovician Bighorn Formation. Approximately 80 m to the north–northwest, the formation rests on the Beartooth Butte Formation, although both the Maywood and upper Beartooth Butte weather recessively and are largely covered (Fig. 1C). The Maywood Formation is sharply gradationally, or slightly unconformably, overlain by the Frasnian (Upper Devonian) Jefferson Formation (Fig. 1D).

We measured a section through the Maywood Formation on a centimeter scale using a tape, and a covered interval using a Jacob Staff. Detailed sedimentological data and palynological samples were collected throughout the formation. Four samples of organic rich shale, calcareous shale, and calcisiltite were collected at 3.2 m, 3.5 m, 4.2 m, and 4.53 m from the Maywood Formation for palynological analysis. Samples were processed by the Global Geolab in Medicine Hat, Alberta, Canada, and by one of us (Mercedes di Pasquo) at the Centro de Investigaciones Científicas y Tecnológicas de Transferencia a la Producción (CICYTTP-CONICET-ER-UADER), Diamante, Entre Ríos Province, Argentina. Methodologies followed at each laboratory are summarized herein.

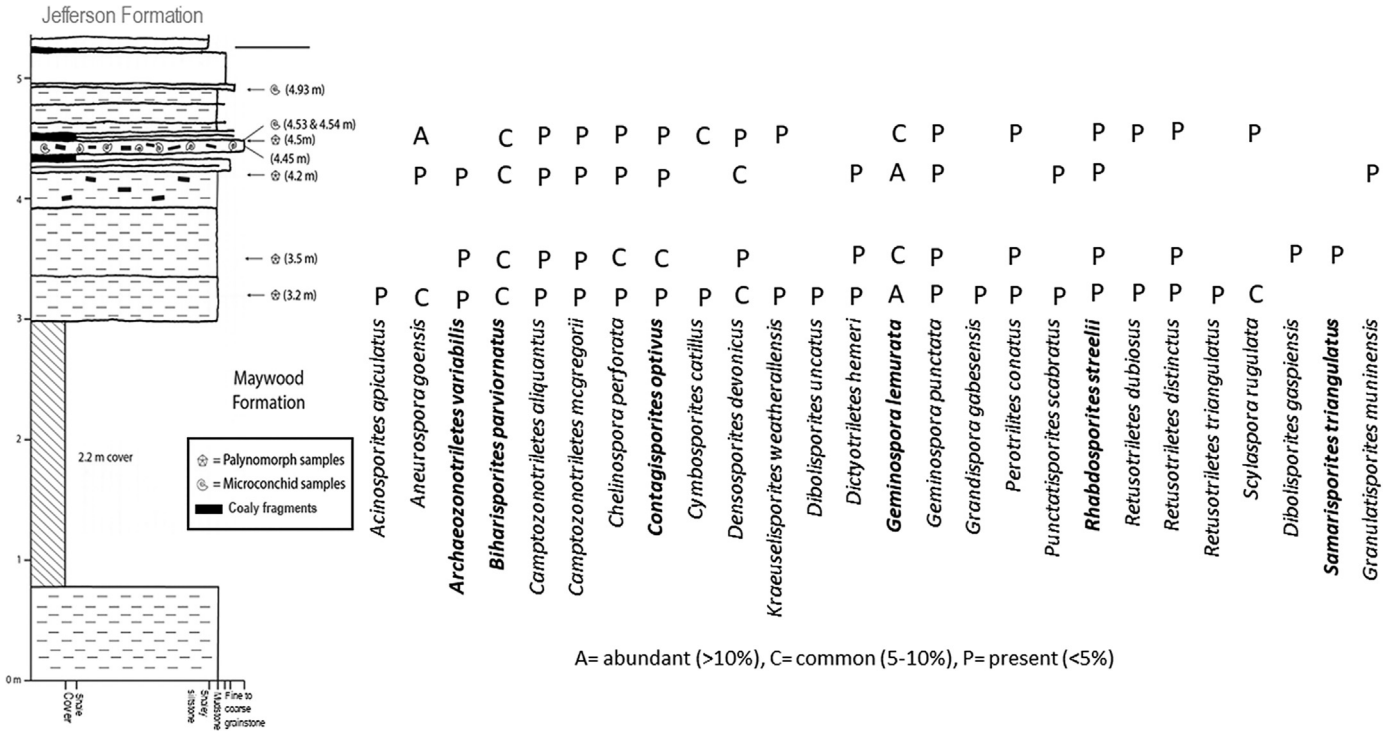

Fig. 2. Abundance of palynotaxa alongside the stratigraphic column of Maywood Formation at Cottonwood Canyon, WY. Bold taxa are biostratigraphically significant. The vertical axis is stratigraphic height (in meters). Black rectangles represent large pieces of coal fragments and plant debris. Numbers in brackets indicate stratigraphic position of microconchid and palynologic samples.

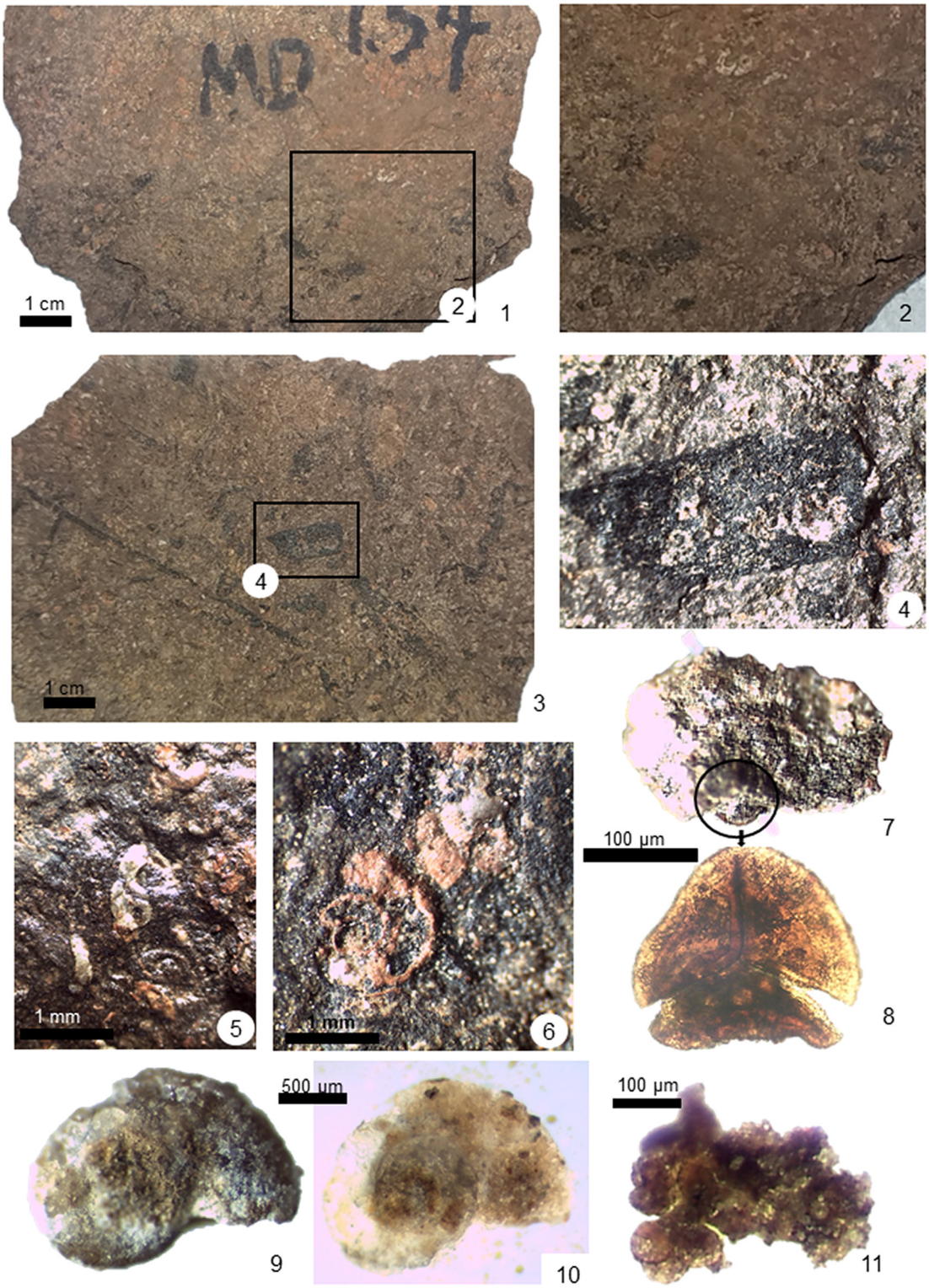

Plate I. Fossils of the rock sample at 4.53 m (CICYTTP-Pl 2608). **1–2**. Upper surface (exposed) of the slab bearing coiled microconchids and black plant debris enlarged in 2**. 3**. Back surface of the same slab showing small microconchids and black plant debris (coaly compressions), one in a square enlarged in fig. **4**. **5–6**. Microconchids from the same slab surfaces. **7**. Fragment of microconchid (c. 1 mm) bearing a small megaspore (see circle and arrow), the former released from the surface of the slab using a thin nail and water. **8**. *Contagisporites optivus* (Tchibrikova) Owens (megaspore of 220 µm, CICYTTP-M 548) released from the microconchid (after taking the picture in fig. **7** using the thin nail and water into a Petry box under the stereomicroscope. **9-11**. Fossils recovered from a piece of rock sample at 4.53 m after applying Sodium Hexametaphosphate (SH). **9-10**. Microconchid bearing fine grains of sand (**9**) removed using thin nail and brush with water into a Petry box under the stereomicroscope revealing the siliceous nature of the specimen (**10**). **11**. Cluster of microspores.

In Canada, standard palynologic maceration was followed using HCl (10%) and HF (70%), and several washes with distilled water allowed the neutralization of residues, which were sieved using 5 µm meshes. Four slide mounts were made using a drop of residue mixed with one drop of polyvinyl alcohol. After drying, one drop of clear casting resin was added, and the cover slip turned and sealed. The residues were

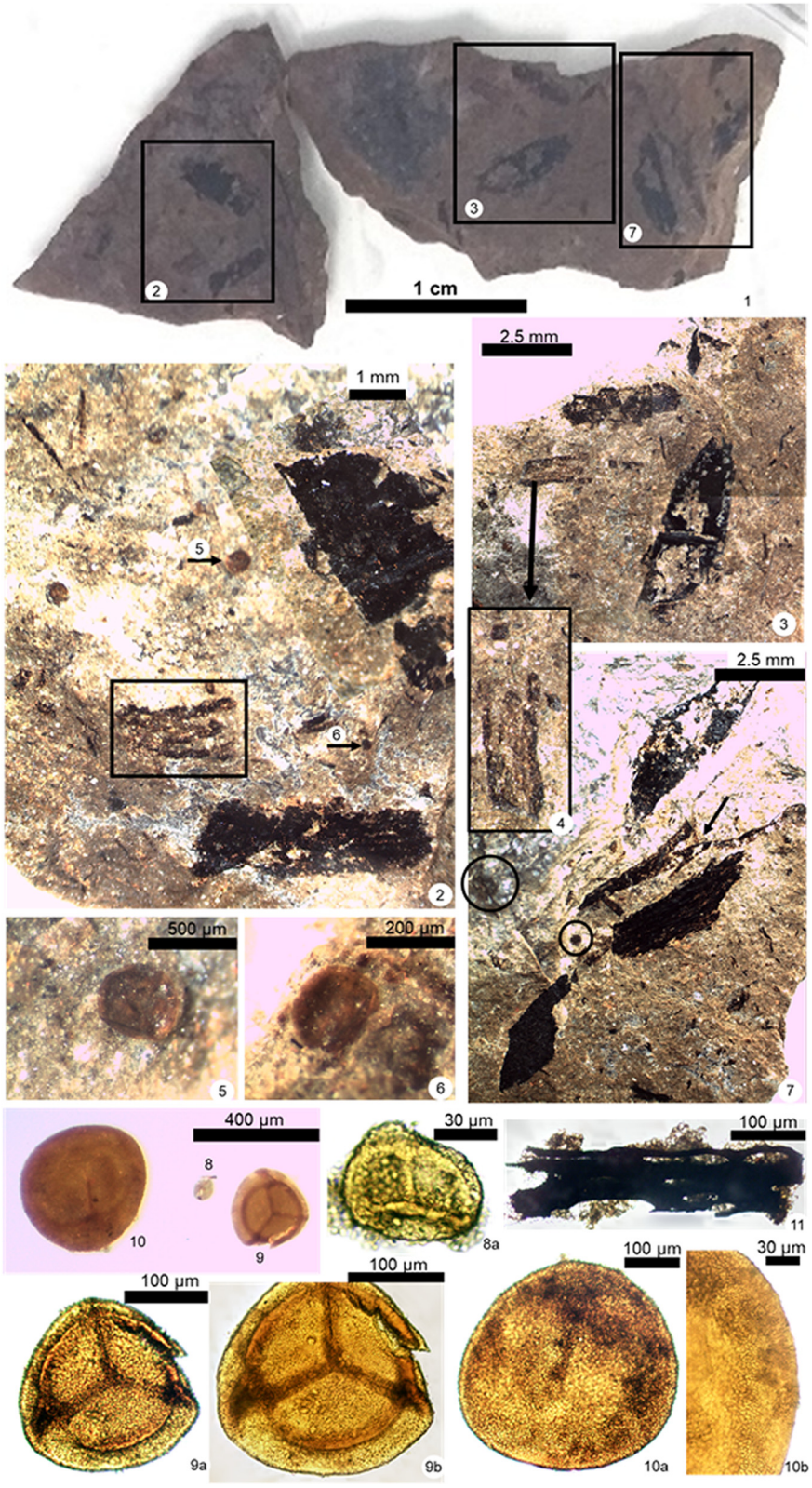

Plate II. 1–7. Plant fossils exposed on the surface of two pieces of the sample at 4.2 m (CICYTTP-Pl 2607) after applying Sodium Hexametaphosphate (SH) during two weeks illustrated into a Petry box under the stereomicroscope. **1.** Surface of the slabs exposing coaly compressions (black) of plant debris and megaspores enlarged in figs. 2 – 7 indicated by squares and arrows respectively. **2**. Surface of rock showing coaly compressions as the one into the square, which is coincident to that in figure 4; two megaspores enlarged in figs. 5 and 6 are indicated by arrows. **3.** In this slab a fusiform sporangium shown in the central right part of the figure. **4**. A coaly specimen indicated by an arrow in fig. 3, is herein interpreted as possible distal fragments of leaves. **7**. A fusiform sporangium in the upper right part and megaspores (encircle) and coaly fragments of stems, one showing a bifurcation (arrow). **8–11.** Spores and tracheids picked from the SH residue using a thin nail into a Petry box. **8**. Microspore (*Aneurospora*) illustrated under the stereomicroscope. **8a.** The same specimen illustrated under the microscope after being mounted in a non-permanent slide using X40 objective. **9**. *Contagisporites optivus* (Tchibrikova) Owens under stereomicroscope. **9a–9b**. The same specimen illustrated under the microscope with X10 (9a) and X40 (9b) magnifications. **10**. *Biharisporites parviornatus* Richardson illustrated under stereomicroscope. **10a–10b**. The same specimen illustrated under the microscope with X10 (10a) and X40 (10b) magnifications. **11.** Tracheid illustrated under the microscope (X10).

oxidized with 3 ml of Schultz solution in a hot bath for a short time, and after washing and centrifuging until neutralization, a 10% solution of NH_4OH was added. The residues were then placed in hot water bath for two minutes and washed three to four times. Two sets of slides were created: one set with oxidized residues (3.5 m and 4.2 m) and another with oxidized residues (3.2 m and 4.5 m) stained with a drop of Bismarck Brown Y. Slides and residues and sample material were delivered to Argentina for palynologic analysis (cf. Zatoń et al., 2021).

In Argentina, standard palynologic maceration of the samples was followed applying HCl (25%) and HF (40%), and several washes with distilled water allowed the neutralization of residues, which were sieved using 10 and 25 μm meshes and slides mounted with Trabasil. The microscopic analysis was performed using light microscopes Nikon E200 and Leica DM500 (bearing a fluorescence device) and pictures were taken with video cameras Labomed 5.0 and Amuscope 14 Mp, respectively. Megaspores and microspores were picked directly from those residues in a Petry dish using the stereo microscope Leica EC3 bearing a Leica video camera (3 Mpx). Selected specimens were mounted in porta-coverslip with water to take optic and fluorescence images, and after being transferred to stubs, SEM images of unmetallized samples were taken under low vaccum with a Phenom Pro (see di Pasquo and Vilá, 2019). Additionally, selected pieces of rocks of each sample were processed using Sodium Hexametaphosphate, and after two weeks they were analyzed under the stereomicroscope in the aforementioned manner. Materials housed were labeled under the acronym CICYTTP-Pl for residues and slides of the rock samples (CICYTTP-Pl 2605 at 3.2 m up to 2608 at 4.53 m), and CICYTTP-M for mega-microspore specimens picked from residues (di Pasquo and Silvestri, 2014).

4. Results

4.1. Mesofossil remains

From the four samples processed in two different laboratories, there are four palynoassemblages with well preserved palynomorphs. Palynofacies features of all forms are analyzed and described below. From each organic residue individual specimens of microspores and megaspores were picked and illustrated with optic and fluorescence and SEM microscopes (Plates I–VIII).

A survey of the four rock samples under the stereomicroscope allowed recognition of various plant forms and other organic particles. The samples at 3.2 m and 3.5 m show scarce plant remains, whereas those at 4.2 m and 4.53 m reveal abundant plant remains, megaspores, and microconchids, all observed under the stereomicroscope. After applying Sodium Hexametaphosphate to selected pieces of rocks at 4.2 m and 4.53 m, the survey of those at 4.2 m exhibit plant remains that include fusiform sporangia, fragmented leaves (likely their distal portion) and stems (possibly ultimate bifurcated axes), as well as megaspores (*Contagisporites optivus, Biharisporites parviornatus*), microspores, and tracheids (Plate II). A few scales and teeth of fishes are present in the 4.2 m sample, and on the 4.53 m rock slabs microconchids are also abundant along with megaspores and plant remains (Plate I).

The plant remains are similar to the Archaeopteridalean *Archaeopteris roemeriana* (Göppert) Stockmans, which was described and illustrated by Kenrick and Fairon-Demaret (1991) and Fairon-Demaret et al. (2001), and *A. macilenta* (Lesquereux) Carluccio et al., 1966 (see also Beck, 1971). Guo and Wang (2009, 2011) reinvestigated the anatomy of *A. macilenta* from the Frasnian of South China as well as in Russia and North America, and provided a full comparison with *A. halliana (Göppert) Dawson* (= *A. roemeriana*), the more dominant form during the Famennian in the same region and also in Europe and North America.

Following Guo and Wang (2011), *A. macilenta* and *A. halliana* (*A. roemeriana*) differ in having laminated and non-laminated fertile leaves, and vegetative leaves similar in size (less than 2 cm in length), which have entire and slightly uneven and deeply dissected margins, respectively. However, they share many features, such as tree habit, branching system (pseudomonopodial stem with penultimate and ultimate axes), and leaf arrangement (spirals on penultimate and ultimate axes). We presently assign the specimens illustrated in Plate II to *Archaeopteris* sp., as the anatomic details of leaves were not observed in our material. Fairon-Demaret et al. (2001) suggested that non-laminated fertile leaves of *A. roemeriana* may be more efficient for wind dispersal of spores and for good control of water loss by transpiration. This reproductive organ may help better cope with dry and stressful periods of a lower water table. The vegetative leaves of *A. halliana* (*A. roemeriana*) perhaps result in more water loss than those of *A. macilenta*.

4.2. Palynology

The four palynoassemblages (Fig. 2) included amorphous organic matter (60–80%), a low diversity assemblage of well-preserved trilete spores (15–30%), and low levels (5%) of phytoclasts (tracheids) and indeterminate organic particles. Pyrite (mostly euhedral crystals) is present in low abundance in the exine of spores and embedded into AOM (lumps of fibrous and granular- types), in sample CICYTPP-Pl 2606.

Geminospora lemurata is quantitatively dominant (single specimens and tetrads) in the four samples, whereas other species of microspores (e.g., *Camptozonotriletes aliquantus*, *Camptozonotriletes mcgregorii*, *Chelinospora perforata*, *Densosporites devonicus*, *Geminospora punctata*) and megaspores vary in their abundances. The remaining taxa are present in variable amounts in a single sample (Fig. 2). There is a low abundance of algal specimens, including *Dictyotidium* sp. (Plate III, 1), a prasinophycean of marine–brackish affinity, and other indeterminate algal remains. These were best revealed under fluorescence, especially those with brilliant yellow color embedded in dark orange AOM lumps (Plate III). Among them, there are spheroidal forms (*Leiosphaeridia*), large tubular specimens (Plate III, 7–8), *Quadrisporites* sp. (Plate III, 2) of brackish to marine affinity, and coenobia with planar sheets of thin-walled equant cells (Plate III, 3–6) that closely resembles *Musivum gradzinskii* Wood and Turnau (2001), a hydrodictyacean chlorococcalean alga of fresh-water affinity.

5. Systematic palynology

Megaspore and microspore species in this section are organized in alphabetical order by genera. Their evaluation was enhanced by observations made using fluorescence and scanning electron microscopes (SEM) (Plates IV–VIII). Botanical affinity follows Balme (1995), Taylor et al. (2009), or specific references cited below. The global biostratigraphic distribution for each taxa is also provided.

5.1. Megaspores

Genus: **Biharisporites** Potonié, 1956

Type species: *B. spinosus* (Singh) Potonié, 1956

Botanical affinity: Progymnosperm Archaeopteridales (*Archaeopteris halliana*; *Archaeopteris macilenta* (*Biharisporites parviornatus*, Richardson, 1965); *Tanaitus furchihasta* Krassilov et al. (1987), see Balme, 1995; Marshall, 1996a; Fairon-Demaret et al., 2001; Guo and Wang, 2011).

Diagnosis: Trilete megaspore camerate, with circular to subtriangular amb, intexine frequently not well defined, trilete mark bearing variably delimited curvatures, smooth to chagrinate contact areas, and outside with cones, spines, mucronate warts (biform) mainly fused of variable size and density.

Comparison: *Rhabdosporites* Richardson, 1960 (Givetian of England) is a quite similar trilete, circular to sub-triangular, camerate microspore–megaspore distinguished by well-defined smaller and thicker intexine. It has thin exoexine sculptured outside the contact areas in general, with cones and grains and other elements, such as bacula and spines, of small size less than 2 μm and variable density

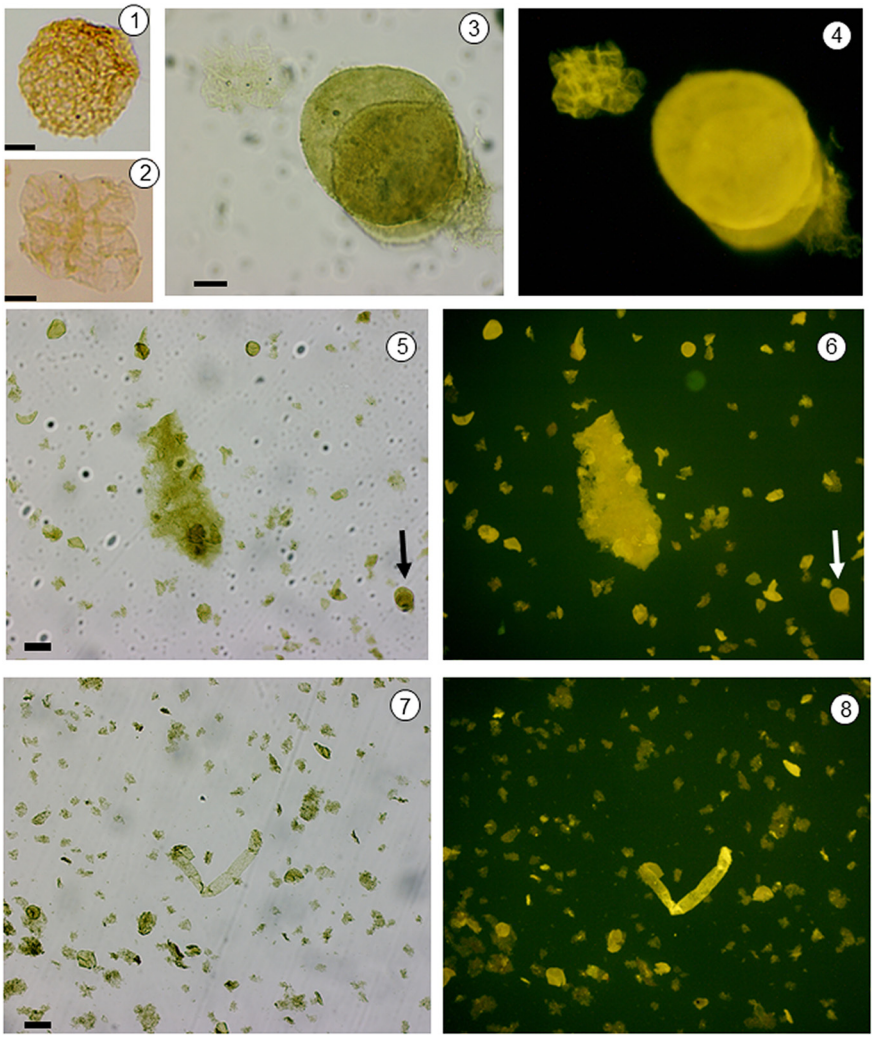

Plate III. 1. *Dictyotidium* sp., CICYTTP-Pl 2605-R3823–1C-ox EF O29. **2**. *Quadrisporites* sp., CICYTTP-Pl 2608-R3823-4A-ox EF M30/1. **3–6**. Palynofacies. 3–4. *Geminospora lemurata* Balme emend. Playford and algal colony marked with arrow in figs. 5–6, where AOM and other phyto-debris are also illustrated under white (3, 5) and fluorescent lights (4, 6), CICYTTP-Pl 2608-R3823-4B-ox (oxidized and stained residue) EF V13/1. **7–8**. Palynofacies. Large tubular form and spores and AOM under white (7) and fluorescent lights (8) CICYTTP-Pl 2607-R3823-3A-ox (oxidized residue), EF O12/3. Scale bar 10 μm in figs. 1–4 and 100 μm in the remaining.

(see also Marshall, 1996a). *Corystisporites* Richardson, 1965 is described as a non camerate, subcircular–subtriangular microspore with defined contact areas that are generally not ornamented; they have a trilete with prominent lips (gulate-like), and are ornamented by longer spiny processes of sharp ends, or they bear a thorn (see also McGregor and Camfield, 1982).

Biharisporites parviornatus Richardson, 1965

Plate II, 10, Plate IV, 1–9, Plate V, 1–14.

Description: Trilete camerate megaspore, subcircular to oval amb. Intexine indistinct, thin and smooth (Plate IV, fig. 8, Plate V, figs. 5, 14), with variable outline between circular to oval. Trilete mark short, somewhat with thin lips, c. ¼ to ½ of the radius, and curvatures distinct (Plate IV, figs. 3, 4, 7, 9, Plate V, fig. 7, 9, 10, 12) or indistinct, delimiting smooth to infrapunctate contact areas (Plate IV, figs. 3, 9, Plate V, fig. 10, 14). Exoexine slightly thicker with spongeous microstructure, somewhat folded bearing discrete and fused ornamentation composed of closely packed small grana, warts, baculae, and biform elements, lesser than 5 μm in width and height (Plate IV, figs. 2, 9, Plate V, figs. 6, 13, 14).

Dimensions (30 specimens measured): Maximum equatorial diameter 240(400)600 μm.

Comparison: *Biharisporites ellesmerensis* Chaloner, 1959 has very similar ornamentation but is smaller and has elevated labra. *Biharisporites* sp. 1 Steemans et al. (2011, Plate II, figs. 4–10) shares morphologic features especially with our specimen illustrated in Plate V, figs. 3, 7, 10, 14, so its assignment to *B. parviornatus* cannot be discarded. *Biharisporites lugardonii* Steemans et al. (2011) only differs in having a spinose ornamentation. *Contagisporites optivus* bears a well- defined smaller central body with ridge-like curvaturae marked by the lipped-laesurae closer to the equatorial margin (Marshall, 1996a; Breuer and Steemans, 2013).

Geographic and stratigraphic distribution: upper Eifelian–Givetian of western Europe, North America, South America (Richardson and McGregor, 1986; di Pasquo, 2007; di Pasquo et al., 2009 [suppl. Online material]; Turnau, 2014), Australia (Grey, 1991).

Genus: **Contagisporites** Owens, 1971

Type species: *Contagisporites optivus* (Tchibrikova) Owens, 1971.

Botanical affinity: Progymnosperm Archaeopteridales (Pettit, in Mortimer and Chaloner, 1967; Balme, 1995; Marshall, 1996a; Turnau, 2014).

Contagisporites optivus (Tchibrikova) Owens, 1971

Plate I, 8, Plate II, 9, Plate VI, 1–12, 15, 16.

Description: Trilete radial megaspore, camerate, subcircular to subtriangular amb, commonly with a limbus, up to 12 μm wide. Laesurae distinct with connected raised lips by well-defined near-equatorial perfect curvatures. Exoexine attached to the smaller inner body (intexine) over only part of the proximal surface, completely

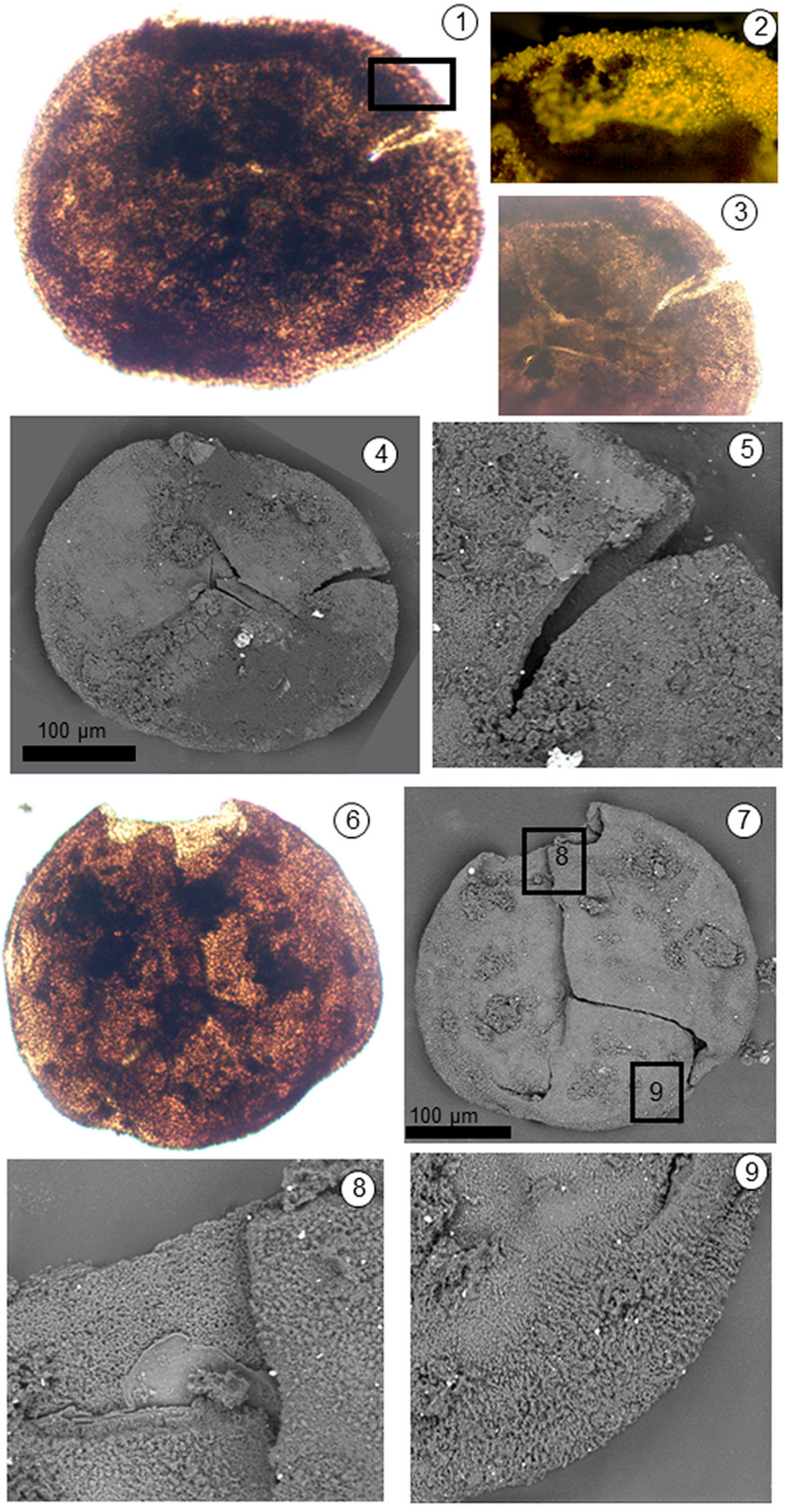

Plate IV. 1–9. *Biharisporites parviornatus* Richardson. Two specimens in figs. 1 and 6 show whole morphologic features, and the remaining pictures under different lights depict details of the proximal face, such as the laesurae and smooth contact areas delimited by slightly marked curvaturae, and small varied ornamentation outside. 1–5. CICYTTP-M 541 (CICYTTP-Pl2608). 6–9. CICYTTP-M 538 (CICYTTP-Pl2605).

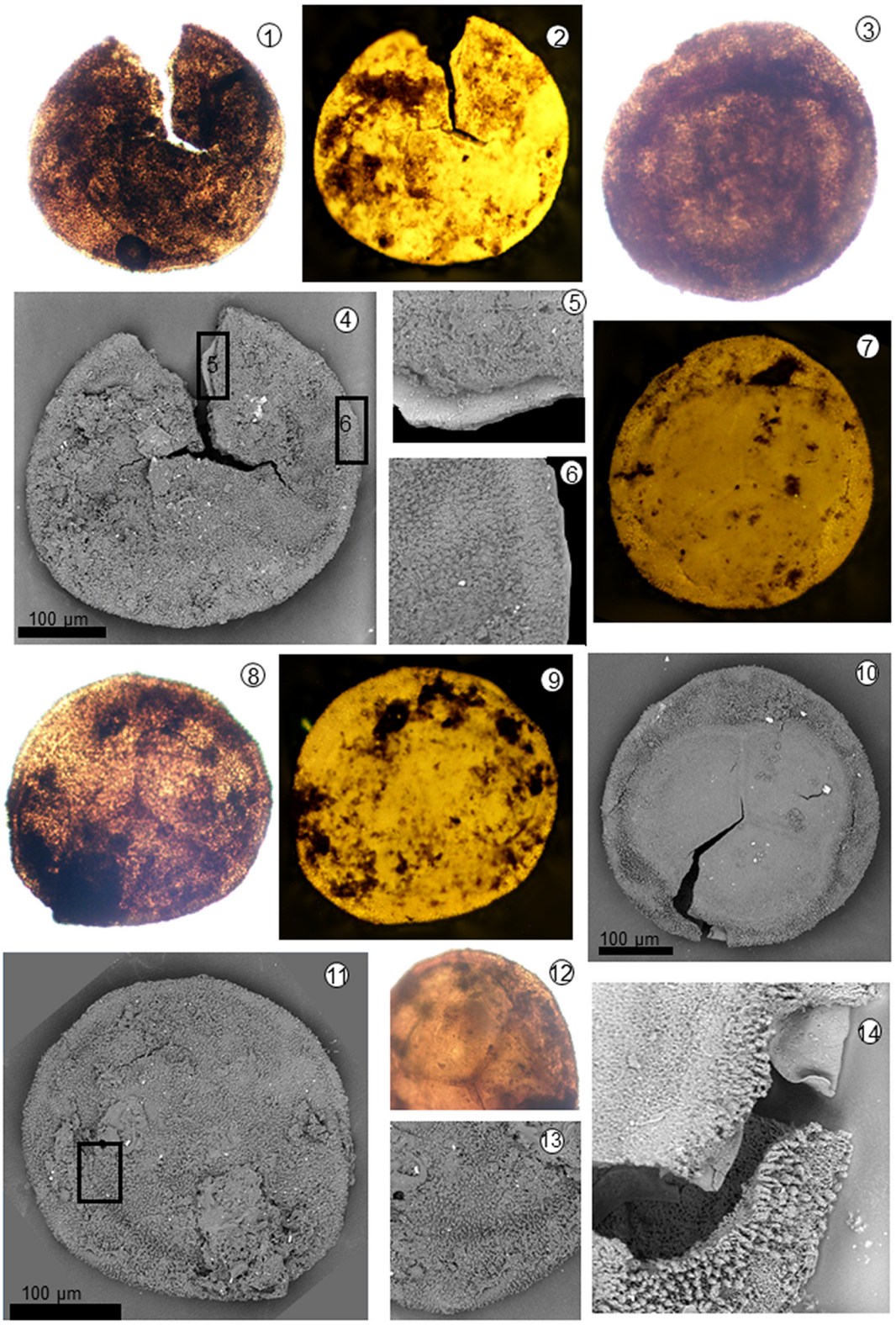

Plate V. 1–14. *Biharisporites parviornatus* Richardson. Three specimens in figs. 1, 3 and 8 show whole morphologic features, figs. 7, 9, 10, 12 reveal smooth contact areas and curvatures in proximal face, figs. 5 and 14 show the internal structure of exine with thin homogenous intexine and punctate/spongeous exoexine, and remaining pictures depict details of ornamentation in distal face bearing closely packed small varied elementes. 1–2, 4–6. CICYTTP-M 542 (CICYTTP-Pl2608). 3, 7, 10, 14. CICYTTP-M 539 (CICYTTP-Pl2605). 8–9, 11–13. CICYTTP-M 540 (CICYTTP-Pl2605).

separated in the equatorial plane and over the entire distal surface. The inner body thin, laevigate, commonly folded. Ornamentation outside the laevigate contact areas composed of small granules and conate or spinose elements.

Dimensions (10 specimens measured): Equatorial diameter 180 (200)350 μm.

Remark: *Contagisporites optivus* var. *vorobjevensis* (Tchibrikova) Owens, 1971 differenciated mainly from *Contagisporites optivus*

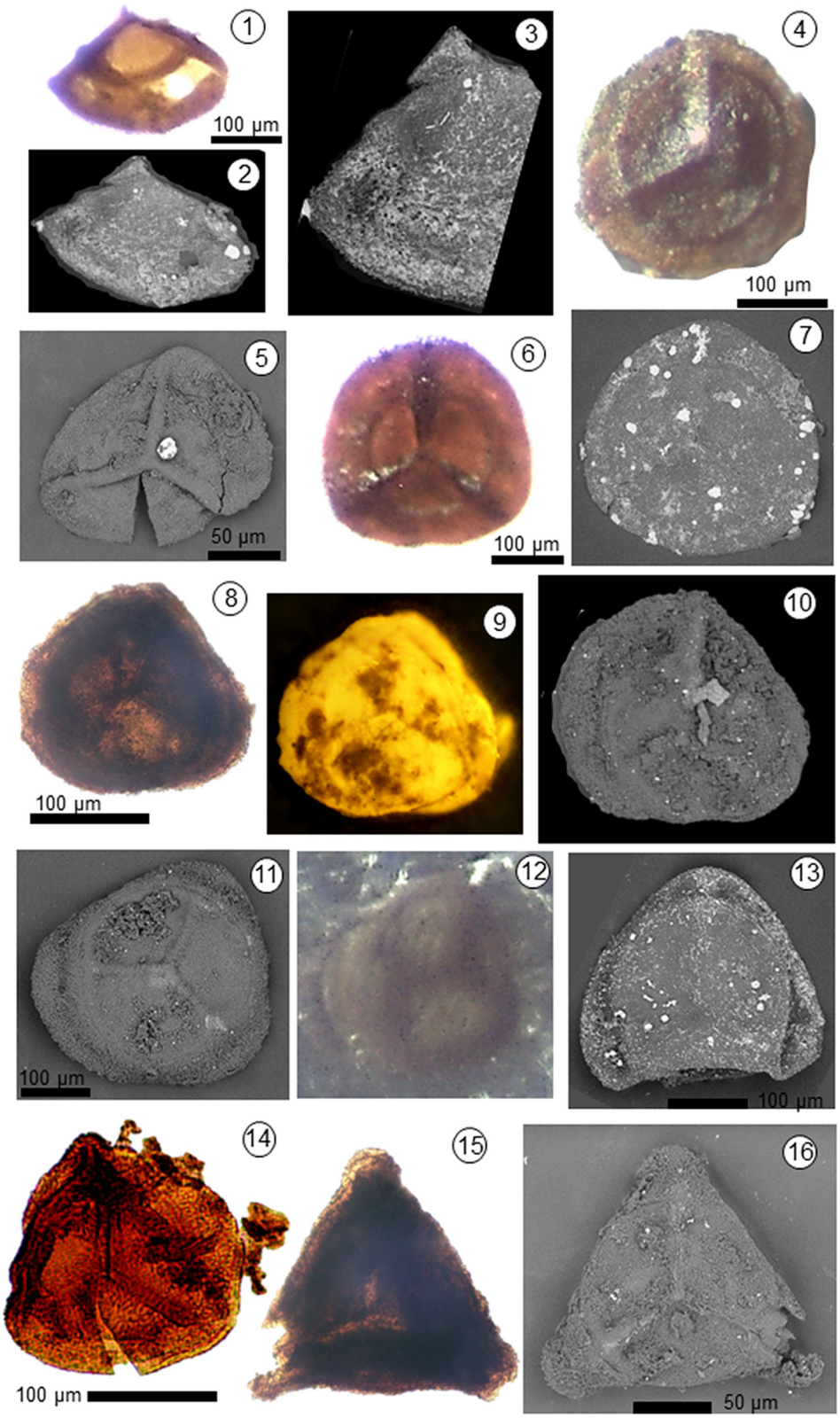

Plate VI. 1–12. *Contagisporites optivus* (Tchibrikova) Owens. 1–3. Lateral compression of a specimen (CICYTTP-M 530 (CICYTTP-Pl 2606) illustrated under stereomicroscope before being transferred to stub for SEM illustration. 4, 7. Specimen showing the general morphologic structure of proximal face illustrated under the stereomicroscope (CICYTTP-M 531 (CICYTTP-Pl 2606). 5. Proximal face of specimen illustrated with SEM (CICYTTP-M 533 (CICYTTP-Pl 2605). 6. Specimen (CICYTTP-M 532 (CICYTTP-Pl 2606) illustrated under stereomicroscope. 8–10. Specimen (CICYTTP-M 535 (CICYTTP-Pl 2608) illustrated with white and fluorescent lights and Scanning electronic micromicroscopes. 11–12. The same specimen (CICYTTP-M 534 (CICYTTP-Pl 2605) showing the general morphologic structure of proximal face illustrated on the stub under the stereomicroscope in fig. 12. **13, 14**. *Rhabdosporites streelii* Marshall. 13. SEM picture of proximal face (CICYTTP-M 537 (CICYTTP-Pl 2607). 14. CICYTTP-Pl 2605-R3823–1D EF M40/3. **15–16**. Abnormal/aberrant specimen most likely of *Contagisporites* illustrated under optic and scanning electronic microscopes (CICYTTP-M 536 (CICYTTP-Pl 2608).

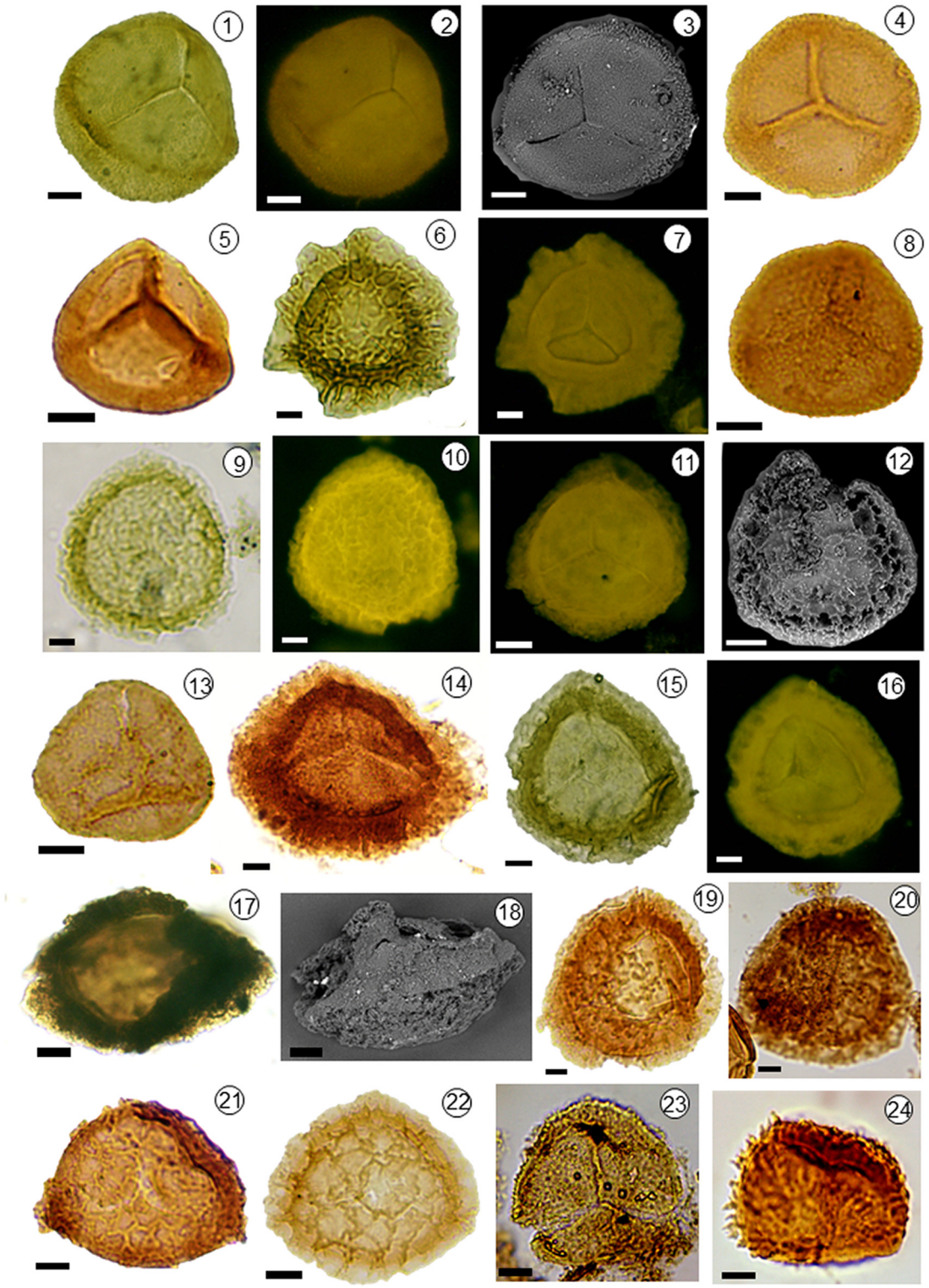

Plate VII. 1–3. *Acinosporites apiculatus* (Streel) Streel. 1–2. Specimen illustrated under white (1) and fluorescent lights (2, proximal face), CICYTTP-Pl 2605-R3823–1A-ox EF S15/1. 3. Specimen illustrated under SEM (proximal face), CICYTTP-M 541 (CICYTTP-Pl 2605). **4**. *Aneurospora goensis* Streel, CICYTTP-Pl 2608-R-3823-4B EF S32/1. **5**. *Archaeozonotriletes variabilis* Naumova emend. Allen, CICYTTP-Pl 2605-R3823-1D EF M40. **6–7**. *Camptozonotriletes mcgregorii* Ravn and Benson, CICYTTP-Pl 2605-R3823-1A EF R27, under white and fluorescent lights. **8**. *Cymbosporites catillus* Allen, CICYTTP-Pl 2608-R3823-4A-ox EF N28. **9–12**. *Camptozonotriletes aliquantus* Allen. 9–10. Specimen illustrated under white (9) and fluorescent lights (10, distal face), CICYTTP-Pl 2608-R3823-4B EF O20/4. 11. Specimen in proximal face under fluorescent light, CICYTTP-Pl 2607-R3823-3A EF K17. 12. Specimen illustrated under SEM (distal face), CICYTTP-M 542 (CICYTTP-Pl 2605). **13**. *Granulatisporites muninensis* Allen, CICYTTP-Pl 2607-R3823-3A EF K21/4.**14–18**. *Chelinospora perforata* Allen. 14. CICYTTP-Pl 2607-R-3823-3A EF N29/1. 15–16. Same specimen showing its proximal face under fluorescent light in 16, R3823-3A-ox EF Q14/1. 17–18. Same specimen illustrated under white light and SEM, CICYTTP-M 543 (CICYTTP-Pl 2608). **19–20**. *Densosporites devonicus* Richardson. 19. CICYTTP-Pl 2607-R3823-3D EF Q25/2 (focus on ornamented distal face). 20. CICYTTP-Pl 2608-R-3823-4A EF O23/2. **21**. *Dictyotriletes hemeri* Breuer and Steemans, CICYTTP-Pl 2607-R-3823-3A EF X20/4. **22.** *Camptozonotriletes aliquantus* Allen (transitional to *D. hemeri*), CICYTTP-Pl 2608-R-3823-4B EF Y54/3. **23**. *Dibolisporites gaspiensis* (McGregor) Breuer and Steemans, CICYTTP-Pl 2606-R3823-2C EF M29. **24**. *Dibolisporites uncatus* (Naumova) McGregor and Camfield, CICYTTP-Pl 2605-R3823–1C-ox EF T25. Scale bars = 10 μm.

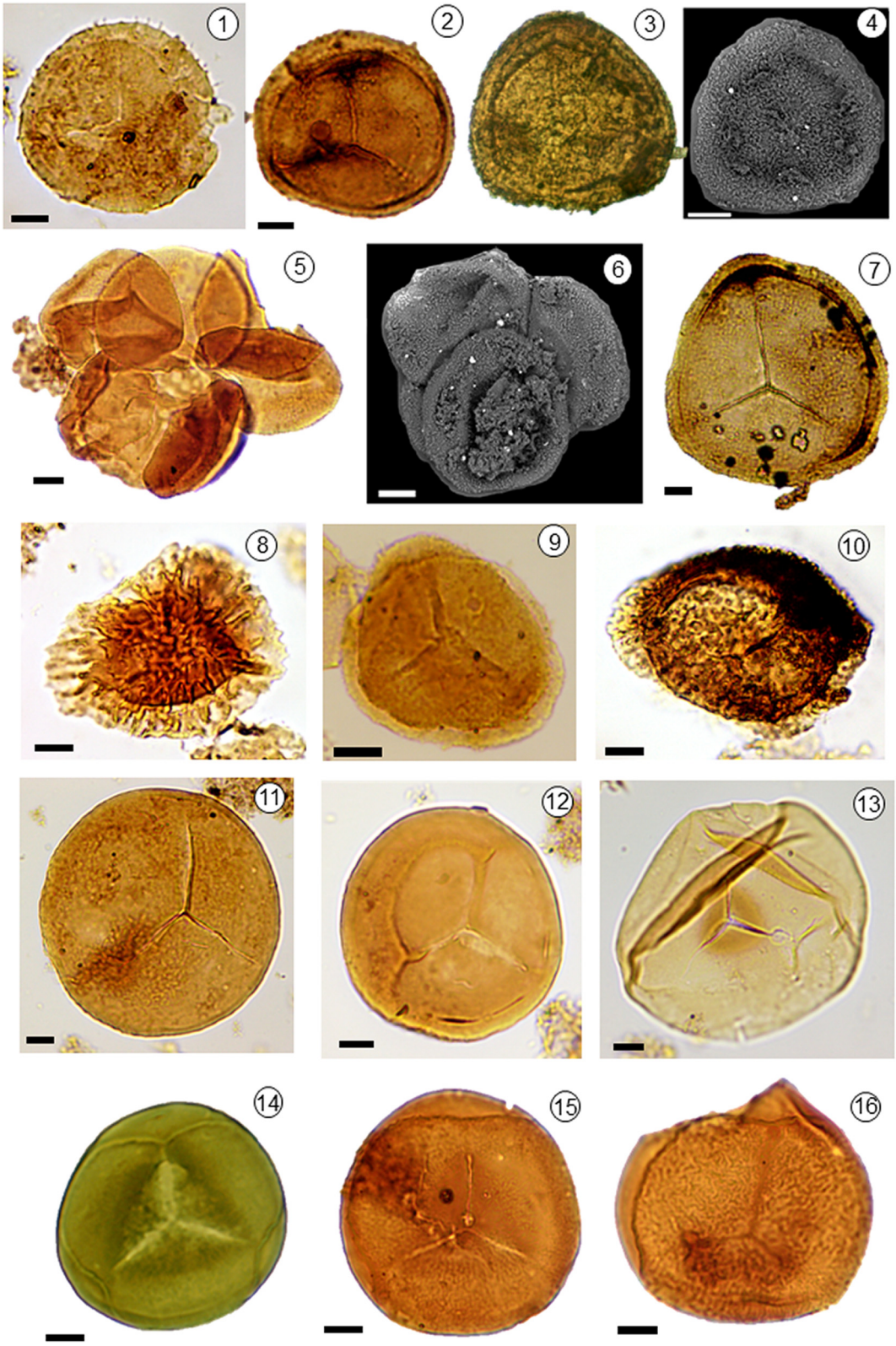

Plate VIII. 1. *Grandispora gabesensis* Loboziak and Streel, CICYTTP-Pl 2605-R3823–1D EF P30/4. **2–6.** *Geminospora lemurata* Balme emend. Playford. 2. CICYTTP-Pl 2606-R3823-2A-ox J17. 3–4. Same specimen illustrated with optic and SEM (distal face), CICYTTP-M 545 (CICYTTP-Pl 2605). 5. Tetrads, CICYTTP-Pl 2605-R3823–1 EF S15. 6. Tetrad (SEM), CICYTTP-M 544 (CICYTTP-Pl 2605). **7**. *Geminospora punctata* Owens, CICYTTP-Pl 2606-R3823-2C EF P30/4. **8**. *Kraeuselisporites weatherallensis* (McGregor and Camfield) nov. comb., CICYTTP-Pl 2605-R-3823-1A EF P39/3. **9**. *Perotrilites conatus* Richardson, CICYTTP-Pl 2608-R3823-4A-ox EF Q29/2. **10**. *Samarisporites triangulatus* Allen, CICYTTP-Pl 2606-R3823-2B EF P29/3. **11**. *Punctatisporites scabratus* McGregor, CICYTTP-Pl 2607-R-3823-3A EF Q12. **12**. *Retusotriletes dubiosus* McGregor, CICYTTP-Pl 2605-R-3823-1A EF M23. **13**. *Retusotriletes triangulatus* (Streel) Streel, CICYTTP-Pl 2605-R3823–1D EF M41/4. **14**. *Retusotriletes distinctus* Richardson, CICYTTP-Pl 2605-R3823–1A EF T16/4. **15–16**. *Scylaspora rugulata* (Riëgel) Breuer et al. 15. CICYTTP-Pl 2605-R-3823-1A EF K41/2. 16. CICYTTP-Pl 2605-R3823–1D EF Q27. Scale bar 10 μm.

(Tchibrikova) var. *optivus* Owens, 1971 by its coarser, low verrucose or blunt pointed conate elements, are grouped herein together in agreement with Breuer and Steemans (2013).

Comparison: *Contagisporites optivus* (Tchibrikova) Owens, 1971 differs from *Rhabdosporites langii* (Eisenack) Richardson, 1960 by its well-developed curvaturae and elevated labra. A pattern of morphologic variations and frequency of *Geminospora lemurata*, *Rhabdosporites langii*, *Rhabdosporites streelii* and *Contagisporites optivus* was documented by Marshall (1996a) from lower Rousay Flagstone of Givetian age to the early Frasnian Eday Flags formations in United Kingdom. The "earlier forms" of *Geminospora lemurata* and *Contagisporites optivus,* in which the curvatural ring is not well-delimited, are also observed in our assemblages (Plate VI).

Geographic and stratigraphic distribution: Cosmopolitan species of the Givetian (*Contagisporites optivus* var. *optivus–Samarisporites triangulatus* Zone of Richardson and McGregor, 1986) and Frasnian (Allen, 1965; Owens, 1971; Chi and Hills, 1976; Whiteley, 1980; Gao, 1981; Grey, 1991; Marshall, 1996a, 1996b, 2000; Marshall et al., 1996, 2011; Turnau and Racki, 1999; Steemans et al., 2011; Breuer and Steemans, 2013; Grahn et al., 2013; Turnau, 2014; Noetinger, 2015; di Pasquo et al., 2015; Berry and Marshall, 2015; Streel et al., 2021; Palynodata, 2006).

Genus: **Rhabdosporites** Richardson emend. Marshall and Allen, 1982

Type species: *Rhabdosporites langii* (Eisenack) Richardson, 1960.

Botanical affinity: Progymnospermaphyta, Aneurophytales (see Marshall, 1996a).

Rhabdosporites streelii Marshall, 1996a

Plate VI, 13–14

Description: Trilete megaspore, camerate, subtriangular to subcircular-oval. Exine with three layers, two inner ones surrounded by exoexine attached in proximal pole. Trilete mark simple straight with lips extended 2/3 of the spore radius, reaching well-defined curvaturae close to the equatorial margin. Intexine thin circular to oval triangular, smooth, slightly darker than the exoexine, which bears a limbus at the margin (Plate VI, fig. 14). Distal and proximo-equatorial surfaces, outside of contact areas, ornamented by small densely packed coni, grana and rods lesser than 1–2 μm.

Dimensions (five specimens measured): Equatorial diameter 190–270 μm.

Comparisons: *Geminospora macromanifesta* (Naumova) Avkhimovitch, illustrated by Tel'nova (2008, pl. 1, fig. 17) from the Givetian–Frasnian of URSS, closely resembles and could be considered conspecific with this taxon.

Geographic and stratigraphic distribution: Givetian, Canada, Europe, Brazil, Libya and Saudi Arabia (see Marshall, 1996a; Marshall et al., 2011; Breuer and Grahn, 2011; Breuer and Steemans, 2013).

5.2. Microspores

Genus: **Acinosporites** Richardson, 1965

Type species: *A. acanthomammillatus* Richardson, 1965.

Botanical affinity: Bryophyta (*Orestovia devonica Ergolskaya, see Balme, 1995*). Lycophyta Protolepidodendrales (*Leclercqia complexa* Banks, Bonamo and Grierson, bearing *Acinosporites lindlarensis*; see Balme, 1995; Wellman et al., 2009; Xu et al., 2011).

Acinosporites apiculatus (Streel) Streel, 1967

Plate VI, 1–3

Description: Spores radial, trilete, amb broadly rounded triangular to subtriangular. Trilete mark distinct; laesurae straight, 2/3 to 4/5 of the spore radius in length, accompanied by thin lips, and their ends slightly fused laterally with the ridge-like curvaturae. Exine of the contact areas slightly thinner than that of the remainder of the spore, surface minutely roughened due to very dense and fine infrastructure. Exine of the remainder of the proximal surface and the entire distal surface densely ornamented with minute, discrete and fused grana, spinae and small mucronate verrucae (lesser than 3 μm). Thickness of the exine at the equator is variable, between 3 and 10 μm, within individual specimens.

Dimensions (four specimens measured): Equatorial diameter 65–100 μm.

Remarks: Streel (1964) defined this species as *Verrucosisporites apiculatus* with a few large specimens 118–150 μm across from the Givetian of Belgium. It was later combined by Streel (1967) to *Acinosporites* despite the smaller size (54–65 μm) of the specimens documented in from Emsian/Eifelian strata of the same country.

Comparison: Owens (1971) described similar large specimens (c. 130–200 μm) as *Apiculiretusispora* sp. A and sp. B, differing by their smaller contact areas and discrete smaller ornamentation.

Geographic and stratigraphic distribution: middle Emsian – Givetian of Europe, Africa, Saudi Arabia, and South America (Melo and Loboziak, 2003; Breuer et al., 2007; di Pasquo, 2007; di Pasquo et al., 2009 [suppl. Online material]; Breuer and Grahn, 2011; Grahn et al., 2013; Breuer and Steemans, 2013, and references therein).

Genus: **Aneurospora** Streel, 1964

Type species: *Aneurospora goensis* Streel, 1964.

Botanical affinity: *Aglaophyton major (Kidston and Lang) Edwards, see Balme, 1995*). Rhyniophyta Rhyniales (*Cooksonia pertoni Lang, see Balme, 1995*). Lycopsida (*Lycopodites oosensis Kräusel and Weyland*), Drepanophycalles (*Asteroxylon mackiei Kidston and Lang*). Progymnospermopsida Aneurophytales (*Aneurophyton germanicum Kräusel and Weyland*, *Aneurospora goensis*, Streel, 1964; see Balme, 1995; Marshall, 1996a), Archaeopteridales (*Archaeopteris roemeriana*, *Aneurospora greggsii* (Mcgregor) Streel in Becker, Bless, Streel, Thorez 1974, see Fairon-Demaret et al., 2001).

Aneurospora goensis Streel, 1964

Plate VII, 4

Description: Trilete acamerate spores with a subcircular amb. A subequatorial proximal region thickened like a dark band equatorial crassitude with comonly ill-defined inner limits and a width that is is also variable, even in the same specimen. Laesurae straight bearing lips with a proximal region laevigate or variously disperse sculpture. Distal region with dense small (lesser than 1 μm) grana, coni, spinae, and biform elements.

Dimensions (six specimens measured): Equatorial diameter 40–63 μm.

Comparison: It is likely conspecific with *Aneurospora extensa* (Turnau and Racki, 1999; Turnau, 2014; Streel et al., 2021).

Geographic and stratigraphic distribution: mainly from the Givetian of Europe and North America (Streel, 1964; McGregor, 1979; Turnau and Racki, 1999; Streel et al., 2021).

Genus: **Archaeozonotriletes** Naumova, 1953 emend. Allen, 1965

Type species: *Archaeozonotriletes variabilis* Naumova, 1953 emend. Allen, 1965.

Comparisons: *Cymbosporites* Allen, 1965 has a variably sculptured cingulum and distal face patina.

Archaeozonotriletes variabilis Naumova, 1953 emend. Allen, 1965

Plate VII, 5

Description: Trilete acamerate, patinate spores with circular to subcircular equatorial amb and frequently preserved in oblique and lateral compressions due to the variable extention of the patina. Laesurae simple, straight, equals 3/4 to full of central area. Exine homogeneous, laevigate to finely punctate, proximally markedly thinner and distally strongly patinate (c. 30% of the total diameter) giving the aspect of an irregular cingulum over proximal surface up to 15–30 μm thick.

Dimensions (three specimens measured): Equatorial diameter 40–65 μm.

Geographic and stratigraphic distribution: worldwide documented in upper Eifelian to Famennian strata (e.g., Gao, 1981; McGregor and

Camfield, 1982; Grey, 1991; Marshall, 1996a; Ottone, 1996; Turnau and Racki, 1999; Melo and Loboziak, 2003; Hashemi and Playford, 2005; Tel'nova, 2008; di Pasquo, 2007; di Pasquo et al., 2009 [suppl. Online material]; Breuer and Grahn, 2011; Marshall et al., 2011, 2017; Breuer and Steemans, 2013; Grahn et al., 2013; Turnau, 2014; Noetinger et al., 2018; Streel et al., 2021).

Genus: **Camptozonotriletes** Staplin, 1960

Type species: *Camptozonotriletes vermiculatus* Staplin, 1960.

Botanical affinity: Pteridophyta (Balme, 1995; Turnau, 2014).

Camptozonotriletes aliquantus Allen, 1965

Plate VII, 9–12, 22.

Description: Trilete spore, zono-camerate, exoexine roundly triangular conformable in outline with the intexine. Laesura straight, simple, 2/3 to almost full length of radius. Proximal face laevigate, and in distal central area, high narrow muri (1–3 μm), develop an imperfect reticulum, which is less defined in the flange. The equatorial margin is quite smooth. Compressional folds common.

Dimensions (five specimens measured): Equatorial diameter 60–75 μm.

Comparison: *Perotrilites pannosus* Allen, 1965 differs by having a proximal-equatorial to distal face ornamented with narrow folds that are anastomosing to form an irregular reticulum and bears small cones or biform elements distally.

Geographic and stratigraphic distribution: Emsian–Givetian of Spitsbergen (Allen, 1965), North America and Europe (McGregor and Camfield, 1976, 1982; Richardson and McGregor, 1986; Breuer and Steemans, 2013; Turnau, 2014; Palynodata, 2006).

Camptozonotriletes mcgregori Ravn and Benson, 1988

Plate VII, 6–7

Description: Trilete zono-cinguli-camerate spore, roundly triangular amb. Trilete mark indistinct, simple, straight, extended up to the boundary between the intexine and lower limit of the cingulum, i.e., inner rim of the flange zone (exoexine). Distal surface bearing granulose to verrucose elements somewhat fused to form irregular rugules.

Dimension (three specimens measured): Equatorial diameter 52–65 μm.

Geographic and stratigraphic distribution: Eifelian of USA and Germany (Ravn and Benson, 1988).

Genus: **Chelinospora** Allen, 1965

Type species: *Chelinospora concinna* Allen, 1965.

Botanical affinity: Uncertain vascular plant (*Bitelaria dubjanskii* Ishchenko and Ishchenko, see Balme, 1995).

Chelinospora perforata Allen, 1965

Plate VII, 14–18

Description: Trilete patinate spore, roundly triangular to subcircular amb, conformable with the central area outline. Laesurae straight, simple to slightly lipped, almost full length of central area. Thin exine laevigate in contact areas, and the remaining thicker patina in proximal to distal equatorial thining to the center of distal face (like a cingulum), microcono-granulate to foveo-reticulate ornamentation.

Dimensions (four specimens measured): Equatorial diameter 58–75 μm.

Comparison: This taxon is closely similar to the cingulate *Densosporites crassus* McGregor (1960) from the Givetian of Canada and the cingulizonate taxa *Samarisporites galeatus* Owens, 1971 from the Frasnian of Canada and *Cristatisporites cariosus* Wicander and Playford, 1985 from the upper Frasnian of USA, which bear mammoid cones and tubercular processes over a foveo-reticulate exoexine.

Geographic and stratigraphic distribution: Emsian-Eifelian of Spitsbergen (Allen, 1965).

Genus: **Cymbosporites** Allen, 1965

Type species: *Cymbosporites cyathus* Allen, 1965.

Comparison: Cymbosporites magnificus (Mcgregor) Mcgregor and Camfield, 1982 was proposed as senior synonym of *C. cyathus* based on the revision of its type material. Although, we agree with Breuer and Steemans (2013) to maintain both taxa separated due to the fact that the former bears verrucae and biform elements that are mainly fused to form rugules, whereas a discrete organization of coni and biform elements predominates in the latter.

Botanical affinity: Barinophytopsida (*Barrandeina dusliana (Krejci) Stur), see Balme, 1995*; Taylor et al., 2009).

Cymbosporites catillus Allen, 1965

Plate VII, 8

Description: Trilete patinate spores with circular, subcircular to subtriangular amb. Laesurae straight, sometimes indistinct, accompanied by thin labra, and extending to or almost to the inner margin of the patina. Exine proximally thin, distally and equatorially patinate, commonly 3–8 μm thick equatorially. Proximal surface laevigate, patina sculptured with densely packed grana, small verrucae or coni, commonly 1–2 μm or less high and wide.

Dimensions (five specimens measured): Equatorial diameter 35–65 μm.

Remark: some specimens exhibit reduced patinate/cingulate construction that intergrade in *Aneurospora goensis*.

Geographic and stratigraphic distribution: Cosmopolitan species of the late Emsian–Frasnian/Famennian (Allen, 1965; Ottone, 1996; Burjack et al., 1987; Loboziak et al., 1988, 1992, 1997; Loboziak and Streel, 1989; Loboziak and Melo, 2000, 2002; Melo and Loboziak, 2003; Ghavidel-Syooki, 2003; di Pasquo, 2007; di Pasquo et al., 2009, [suppl. Online material]; Noetinger and di Pasquo, 2011; Breuer and Steemans, 2013; Noetinger et al., 2018). In Turkey, *Cymbosporites catillus* has been quoted as far back in time as the Silurian (Steemans et al., 1996). Breuer and Steemans (2013) proposed the *Samarisporites triangulatus-Cymbosporites catillus* Zone of the middle–upper Givetian in Saudi Arabia.

Genus: **Densosporites** (Berry) Butterworth et al. in Staplin and Jansonius (1964)

Type species: *Densosporites covensis* Berry, 1937.

Botanical affinity: Lycopsida (Chaloneriaceae, Selaginellales) (Balme, 1995).

Densosporites devonicus Richardson, 1960

Plate VII, 19–20

Description: Trilete zonate spores with rounded-subtriangular or subcircular amb. Laesurae straight, commonly indistinct, extending to the inner edge of the zona. Exine thin in contact areas, considerably thicker distally, extended laterally as a zona bearing a dark inner part (cingulum) of variable width that overlaps the central area. Distal and proximal–equatorial regions sculptured with varied spinae or coni or biform elements (c. 1–10 μm long, 1–5 wide at the base), the smaller and more discrete occurring in the distal polar region. Sculptural elements at the outer edge of the dark zone tend to coalesce.

Dimensions (six specimens measured): Equatorial diameter 57–80 μm.

Remark: despite a smaller range size of the specimens recorded, the morphologic features fit with this taxon.

Comparisons: McGregor and Camfield (1982) and Marshall and Allen (1982) and Breuer and Steemans (2013) considered *Densosporites orcadensis* Richardson, 1965 a junior synonym of the present taxon. *Densosporites concinnus* (Owens) McGregor and Camfield, 1982 is smaller in size and less elongate, with a predominantly pointed sculpture, but it intergrades with extreme variants of *Densoporites devonicus* Richardson, 1960 (McGregor and Camfield, 1982). The specimens illustrated by Tel'nova (2008, pl. 2, fig. 17) as *Densosporites meyeirae* Tel'nova (curiously it does not figure in Palynodata) from the Givetian of Russia are morphologically very similar and could be conspecific with the present taxon.

Geographic and stratigraphic distribution: Eifelian–Frasnian of North America, Europe, Russia (Laurentia) (e.g., McGregor and Camfield, 1982; Loboziak et al., 1990; Avkhimovitch et al., 1993; Marshall et al., 1996; Turnau and Racki, 1999; Marshall, 1996a, 2000; Turnau, 2014) and Libya (Streel et al., 1988; Breuer and Steemans, 2013). It is the eponymous of the mid Eifelian–early Givetian *Densosporites devonicus–Grandispora naumovii* Zone of the Old Red Sandstone Region (Laurentia) by Richardson and McGregor (1986).

Genus: **Dibolisporites** Richardson, 1965.

Type species: *D. echinaceus* (Eisenack) Richardson, 1965.

Botanical affinity: Cladoxylales (*Calamophyton primaevum Kräusel and Weyland*; *Foozia minuta Gerrienne*) (Balme, 1995; Taylor et al., 2009).

Dibolisporites uncatus (Naumova) McGregor and Camfield, 1982

Plate VII, 24

Dimensions (two specimens measured): 52–55 μm.

Comparisons: This taxon is characterized by its proximo-equatorial and distal regions sculptured with a mixture of grana, coni, spinae with blunt, pointed, or widened tips, and less verrucae mostly longer than wider, subcircular or irregular in plan view (c. 9 μm high, 1–4.5 μm wide at base), discrete and fused. *Dibolisporites farraginis* McGregor and Camfield, 1982 has smaller sculptural elements, but intergrades with, *Dibolisporites uncatus* (Naumova) McGregor and Camfield, 1982 within the *Verrucosisporites scurrus* Morphon in Breuer and Steemans (2013).

Geographic and stratigraphic distribution: late Eifelian – Frasnian of North America, Europe, South America, Saudi Arabia (McGregor and Camfield, 1982; Loboziak et al., 1988, 1990; di Pasquo, 2007; di Pasquo et al., 2009 [suppl. Online material]; Noetinger and di Pasquo, 2011; Breuer and Grahn, 2011; Breuer and Steemans, 2013, and their references).

Dibolisporites gaspiensis (McGregor, 1973) Breuer and Steemans, 2013

Plate VII, 23

Dimensions (two specimens measured): Equatorial diameter 48–50 μm.

Geographic and stratigraphic distribution: Emsian – Givetian/Frasnian of Canada, South America, Saudi Arabia (di Pasquo, 2007; di Pasquo et al., 2009 [suppl. Online material]; Noetinger and di Pasquo, 2011; Breuer and Grahn, 2011; Breuer and Steemans, 2013, and their references).

Genus: *Dictyotriletes* Naumova, 1939 ex Ishchenko, 1952

Type species: *Dictyotriletes bireticulatus* (Ibrahim) Potonié and Kremp, 1955.

Botanical affinity: Filicopsida (see Balme, 1995; Turnau, 2014).

Remarks: Trilete acamerate spores, subtriangular amb, characterized by a reticulate equatorial and distal face. Reticulum is perfectly closed.

Dictyotriletes hemeri Breuer and Steemans, 2013

Plate VII, 21

Remark: some specimens of *Camptozonotriletes aliquantus* intergrade with the present species (Plate V, fig. 22).

Dimensions (two specimens measured): Equatorial diameter 57–65 μm.

Geographic and stratigraphic distribution: mid Eifelian–Givetian of Saudi Arabia (Breuer and Steemans, 2013).

Genus: **Geminospora** Balme, 1962 emend. Playford, 1983

Type species: *Geminospora lemurata* Balme, 1962.

Botanical affinity: Lycophyta (*Bisporangiostrobus harrisii* (Chitaley, 1988). Progymnospermaphyta, Archaeopteridales (*Archaeopteris* spp.; *Svalbardia* spp.; *Tanaitus furchihasta*). Uncertain (*Spenopteridium keilhanii Nathörst*) (see Playford, 1983; Balme, 1995; Marshall, 1996 a; Taylor et al., 2009).

Geminospora lemurata Balme, 1962 emend. Playford, 1983

Plate I, 3–4, Plate VIII, 2–6

Dimensions (12 specimens measured): Equatorial diameter 50–65 μm.

Remarks and comparisons: numerous single specimens and tetrads recorded in our four samples allow the interpretion that smaller specimens with a lesser appreciable separation of the two layers (exo-intexine) and smaller ornamentation are likely inmature forms. This fact could have led workers to propose many species of *Geminospora* (e.g. *Geminospora antaxia* (Chibrikova) Owens; *G. extensa* (Naumova) Gao; *G. micromanifesta* (Naumova) McGregor and Camfield; *G. notata* (Naumova) Obukhovskaya; *G. plicata* Owens; *G. svalbardiae* (Vigran) Allen; *G. tuberculata* (Kedo) Allen; *G. vasjamica* (Tchibrikova) Obukhovskaya and Nekriata). Of them, many were considered junior synonyms of *G. lemurata* as discussed by many researchers (e.g., Owens, 1971; McGregor and Camfield, 1982; Playford, 1983; Avkhimovitch et al., 1993; Tel'nova, 2008; Breuer and Steemans, 2013; Turnau, 2014). Some morphologic differences between "early forms" and those well-established *G. lemurata* in the Givetian were described by Marshall (1996a). *Rhabdosporites langii* (Eisenack) Richardson, 1960 has a generally thinner sexine and a less rigid appearance and it is larger.

Geographic and stratigraphic distribution: cosmopolitan species of the Givetian to Famennian (e.g., Allen, 1965; Owens, 1971; Playford, 1983; McGregor and Camfield, 1982; Richardson and McGregor, 1986; Streel and Loboziak, 1987, 1996; Streel et al., 1987; Balme, 1988; Loboziak et al., 1988, 1992, 1997; Chitaley and McGregor, 1988; Grey, 1991; Avkhimovitch et al., 1993; Hartkopf-Fröder and Streel, 1994; Ottone, 1996; Marshall et al., 1996; Turnau and Racki, 1999; Marshall, 1996a, 1996b, 2000; Loboziak and Melo, 2000, 2002; Melo and Loboziak, 2003; Marshall and Hemsley, 2003; Ghavidel-Syooki, 2003; Hashemi and Playford, 2005; di Pasquo, 2007; Tel'nova Tel'nova, 2008; di Pasquo et al., 2009 [suppl. Online material], 2015; Noetinger and di Pasquo, 2011; Marshall et al., 2011, 2017; Breuer and Grahn, 2011; Breuer and Steemans, 2013; Grahn et al., 2013; Turnau, 2014; Berry and Marshall, 2015; Noetinger et al., 2018; Streel et al., 2021). This taxon is used in several zones worldwide including the *Geminospora lemurata–Cymbosporites magnificus* Zone of Richardson and McGregor (1986) from North America (ORS Continent), *G. lemurata–Ancyrospora langi* Zone of Breuer and Steemans (2013) from Saudi Arabia of northern Gondwana, and the *G. lemurata–Chelinospora* ex *gr. ligurata* (LLi) Interval Zone of Melo and Loboziak (2003, Breuer and Grahn, 2011; Breuer and Steemans, 2013) from Brazil, the latter of which is also recognized in Argentina and Bolivia (di Pasquo et al., 2009, 2015; Noetinger and di Pasquo, 2011; Noetinger et al., 2018). In Fig. 4 it is shown the correlations of these zones also with the lower part of the *Geminospora extensa* (Ex) Zone of Avkhimovitch et al. (1993) from Eastern Europe (see also Turnau, 2014).

Geminospora punctata Owens, 1971

Plate VIII, 7

Remark: This taxon differs from other species of the genus due to its discrete negative punctate ornamentation of the exine, which is finely striated at the equator.

Dimensions (six specimens measured): Equatorial diameter 60–75 μm.

Geographic and stratigraphic distribution: widely known from Eifelian/ Givetian–Frasnian (e.g. Owens, 1971; Turnau and Racki, 1999; Loboziak et al., 1988, 1990; Melo and Loboziak, 2003; Ghavidel-Syooki, 2003; Breuer and Grahn, 2011; Grahn et al., 2013; Breuer and Steemans, 2013).

Genus: **Grandispora** Hoffmeister et al., 1955 emend. Mcgregor 1973

Type species: *Grandispora spinosa* Hoffmeister et al., 1955.

Botanical affinity: Filicopsida, Zygopteridales (*Rhacophyton ceratangium Andrews and Phillips;* Balme, 1995).

Grandispora gabesensis Loboziak and Streel, 1989

Plate VIII, 1

Dimensions (two specimens meassured): Equatorial diameter 55–76 μm.

Geographic and stratigraphic distribution: late Emsian-Frasnian of Africa, Saudi Arabia and South America (see Melo and Loboziak, 2003; di Pasquo, 2007; di Pasquo et al., 2009 [suppl. Online material]; Breuer and Grahn, 2011; Breuer and Steemans, 2013, and references therein).

Genus: *Granulatisporites* Ibrahim, 1933 emend. Potonié and Kremp, 1954

Type species: *G. granulatus* Ibrahim, 1933.

Botanical affinity: Rhyniales (*Rhynia gwynne-vaughanii Kidston and Lang*). Lycopsida, Drepanophycales (*Drepanophycus spinaeformis Göppert; see* Balme, 1995).

Granulatisporites muninensis Allen, 1965

Plate VII, 13

Dimensions (three specimens measured): Equatorial diameter 38–45 μm.

Geographic and stratigraphic distribution: Emsian – Frasnian of North America, Europe, Africa, South America (Allen, 1965; McGregor and Camfield, 1982; Richardson and McGregor, 1986; di Pasquo, 2007; di Pasquo et al., 2009 [suppl. Online material]; Noetinger and di Pasquo, 2011; Noetinger et al., 2018).

Genus: **Kraeuselisporites** Leschik, 1956 emend. Azcuy and di Pasquo, 2005

Type species: *K. dentatus* Leschik, 1956.

Comparisons: This genus has a long story of emendments and comparisons, especially with *Indotrirradites* Tiwari, 1964 (see Genera file of fossil spores of Jansonius et al., 2006). We follow herein the amendment proposed by Azcuy and di Pasquo (2005) that extended the generic diagnosis to include trilete acamerate or camerate spores, zonate to slightly cingulizonate, amb subtriangular with margin entire, smooth or slightly ornamented. Trilete with or without labra. Intexine smooth and denser than the zone, proximal face laevigate or with very reduced small ornamentation. Central body at distal face bearing discrete apiculate elements and other types (e.g. grana, baculae, verrucae, biforms-mammoids) occasionally present, being reduced in size and density on the zone. This amendment reaffirms *Indotriradites* as a junior synonym of *Kraeuselisporites*. On the other hand, *Samarisporites* Richardson (1965) is notably considered a junior synonym of *Cristatisporites* Potonié and Kremp, 1954 by Playford (1971). However, *Samarisporites* Richardson (1965) includes forms with a smooth equatorial amb and an irregular extention of the zone, generally larger at radial ends of of the laesurae, with a denser cental body distal sculpture (e.g., coni, cristae, verrucae) and a lesser ornamention on its zone. This prevents its assignment within *Cristatisporites* Potonié and Kremp, 1954, in which the cingulizone and equatorial margin with apiculate elements mostly fused are ornamented. *Densosporites* is characterized by a cingulum, which is a thick equatorial extention of the exoexine, and this is the main difference with *Kraeuselisporites*.

Botanical affinity: Lycophyta (*Azaniadendron fertile* Rayner and *Indotriradites* by Rayner, 1986, Permian of South Africa, see in Balme, 1995).

Kraeuselisporites weatherallensis (McGregor and Camfield) comb. nov.

Plate VIII, 8

1971 *¿Spinozonotriletes* sp. A Owens, p. 58, pl. 18, fig. 2.

1987 *Samarisporites* sp. E Streel and Loboziak, pl. 1, fig. 10.

Basyonym: Densosporites weatherallensis McGregor and Camfield, 1982, p. 35, pl. 7, figs. 7–9 and 14, text-fig. 49.

Description: Trilete zonate spores with rounded-subtriangular or subcircular amb and intexinal body. Laesura arms 3/4 to full radius of body in length, commonly hidden by prominent triradiate exoexinal folds that extend to, or nearly to, the equator. Intexine laevigate, slightly denser than exoexine. Exoexine thin in laevigate contact areas, thicker distally, extended laterally in equatorial plane as a zone about equal in width to the radius of the intexine. Dark ring with indistinct inner and outer limits may be visible around inner edge of zona. Equatorial and distal regions of exoexine bear coni, verrucae, and ± parallel-sided or tapered processes (maximum in width 7 μm at base and 12 μm in lenght) pointed or rounded, many surmounted by a minute spine that may (rarely) be expanded or bifurcate at the tip. Sculptural elements closely spaced at distal pole joining basally in groups or short rows, whereas they are more widely spaced in the zone toward equator, hence, frequently the intexine boundary is obscured.

Dimensions (three specimens measured): Equatorial diameter 65–78 μm.

Remark: despite a smaller range size of the specimens recorded, the morphologic features fit with this taxon.

Comparisons: *Samarisporites* sp. E Streel and Loboziak, 1987 (pl. 1, fig. 10) from the Givetian–Frasnian of Belgium (see also Streel et al., 2021), and *¿Spinozonotriletes* sp. A Owens (1971) from Canada share their main features with the taxon described, and thus considered conspecific. Other specimens of *Samarisporites* sp. E illustrated by Loboziak et al. (1988, pl. 7, fig. 14) and Loboziak et al., 2000 (pl. 2, fig. 13) from Brazil and by Loboziak and Streel (1989, pl. 4, fig. 9) from Libya, also belong to the species herein. *Cristatisporites deliquescens* (Naumova) Arkhangelskaya illustrated by Obukhovskaya et al. (2000, pl. 1, fig. 1) from the Frasnian of Russia, reassigned to Samarisporites triangulatus by Streel et al. (2021), differs in having more ornamented zone with apiculate elements present in the equatorial margin. *Grandispora megaformis* (Richardson) McGregor, 1973 is a larger azonate camerate species.

Geographic and stratigraphic distribution: upper Eifelian – Givetian of Belgium, Brazil, Libya (Loboziak et al., 1988, 2000; Loboziak and Streel, 1989).

Genus: **Perotrilites** Couper, 1953 emend. Evans, 1970

Type species: *Perotrilites granulatus* Couper, 1953.

Remarks: This genus includes forms bearing a thin irregular zone with two-layer central body (camerate), distally ornamented with discrete and fused grana, apiculate elements, and/or small warts (see McGregor and Camfield, 1982).

Botanical affinity: Pteridophyta, Rhacophyton (Streel and Scheckler, 1990).

Perotrilites conatus Richardson, 1965

Plate VIII, 9

Dimensions (three specimens measured): Equatorial diameter 63–78 μm.

Geographic and stratigraphic distribution: upper Eifelian – Givetian/Frasnian, Europe (Richardson, 1965; Streel, 1972; Turnau, 1996, 2014), North America (McGregor and Uyeno, 1972; McGregor, 1979; Whiteley, 1980; Richardson and McGregor, 1986; see more in Palynodata).

Genus: **Punctatisporites** Ibrahim, 1933 emend. Potonié and Kremp, 1954

Type species: *Punctatisporites punctatus* Ibrahim, 1933.

Botanical affinity: Several primitive vascular plants (Rhyniales, Trimerophytales, Barinophytopsida, Zosterophyllopsida, see Balme, 1995).

Punctatisporites scabratus McGregor, 1960

Plate VIII, 11

Dimensions (3 specimens measured): Equatorial diameter 70–85 μm.

Geographic and stratigraphic distribution: Frasnian, Canada (McGregor, 1960).

Genus: **Retusotriletes** Naumova emend. Streel, 1964

Type species: *Retusotriletes simplex* Naumova, 1953.

Botanical affinity: Several primitive vascular plants (Rhyniales, Barinophytopsida, Drepanophycales, Zosterophyllopsida, see Balme, 1995). Phaeophyta (*Protosalvinia*) and Bryophyta (see Balme, 1995; Taylor et al., 2009).

Retusotriletes dubiosus McGregor, 1973
Plate VIII, 12
Dimensions (two specimens measured): Equatorial diameter 50–65 μm.
Comparisons: Retusotriletes communis Naumova, 1953 illustrated by Avkimovitch et al. (1993, pl. 19, fig. 14) from Middle to Upper Devonian of URSS and *Retusotriletes pychovi* Naumova, 1953 in Avkimovitch et al. (1993, pl. 20, fig. 7) closely resemble this taxon.
Geographic and stratigraphic distribution: Emsian – Frasnian, North America, Europe, Russia, China, Iran, Australia (see Richardson and McGregor, 1986; Hashemi and Playford, 2005; Palynodata, 2006).
Retusotriletes distinctus Richardson, 1965
Plate VIII, 14
Dimensions (three specimens measured): Equatorial diameter 75–90 μm.
Comparison: *Retusotriletes* sp. 1 in Breuer and Steemans (2013, fig. 38.J–L) slightly differs in having less distinct curvatures.
Geographic and stratigraphic distribution: cosmopolitan, Eifelian – Frasnian (e.g. Richardson and McGregor, 1986; Balme, 1988; Turnau, 2014; Palynodata, 2006).
Retusotriletes triangulatus (Streel) Streel, 1967
Plate VIII, 13
Dimensions (three specimens measured): Equatorial diameter 62–78 μm.
Comparisons: Leiotriletes nigratus Naumova illustrated by Tel'nova (2008, pl. 4, fig. 10) and *Calamospora atava* (Naumova) McGregor (1973) are probably conspecific taxa.
Geographic and stratigraphic distribution: Devonian of Europe, North America, Libya, Saudi Arabia, China (e.g. Gao, 1981; Streel et al., 1988; Turnau and Racki, 1999; Wellman, 2006; Breuer and Grahn, 2011; Breuer and Steemans, 2013 and references herein; Turnau, 2014; Palynodata, 2006).

Genus: **Samarisporites** Richardson, 1965
Type species: *S.* (*Cristatisporites*) *orcadensis* (Richardson) Richardson, 1965.
Botanical affinity: Barinophytopsida (*Barrandeina dusliana* (Krejci) Stur, see Balme, 1995). Uncertain plant between trimerophytes and progymnosperms (*Oocampsa catheta* Andrews, Gensel and Kasper, see Balme, 1995; Taylor et al., 2009).
Comparisons: *Samarisporites* Richardson (1965) is notably considered as a junior synonym of *Cristatisporites* Potonié and Kremp, 1954 by Playford (1971). However, *Samarisporites* Richardson (1965) includes zono-camerate forms with an equatorial smooth amb and an irregular extention of the zone that is generally larger at radial ends of the trilete mark. In addition, it has distal sculpture of the central body (e.g., coni, cristae, verrucae), mainly over its central body surface, and bears a slightly different ornamentation in its flange and equatorial margin. Therefore, on these grounds we maintain them as separate genera (see also *Kraeuselisporites* herein).
Samarisporites triangulatus Allen, 1965
Plate VIII, 10
Dimensions (three specimens measured): Equatorial diameter 60–68 μm.
Geographic and stratigraphic distribution: cosmopolitan species of the middle to upper Givetian to Famennian (Allen, 1982; Richardson and McGregor, 1986; Streel et al., 1987; Loboziak et al., 1988, 1990; Balme, 1988; Grey, 1991; Avkhimovitch et al., 1993; Marshall et al., 1996, 2011; Ottone, 1996; Turnau and Racki, 1999; Melo and Loboziak, 2003; Hashemi and Playford, 2005; di Pasquo, 2007; di Pasquo et al., 2009 [suppl. Online material]; Breuer and Grahn, 2011; Noetinger and di Pasquo, 2011; Breuer and Steemans, 2013; Turnau, 2014; Noetinger et al., 2018; Streel et al., 2021).

Genus: **Scylaspora** Burgess and Richardson, 1995
Type species: *Scylaspora scripta* Burgess and Richardson, 1995.
Botanical affinity:?Rhyniopsida (Wellman, 1999).
Scylaspora rugulata (Riëgel) Breuer et al. 2007
Plate VIII, 15–16
Dimensions (three specimens measured): Equatorial diameter 60–75 μm.
Geographic and stratigraphic distribution: Eifelian–Frasnian, North America, Europe, Libya, and Brazil (Breuer et al., 2007; Braman and Hills, 1992; Breuer and Grahn, 2011; Marshall et al., 2011; Breuer and Steemans, 2013 and references herein; Turnau, 2014; Streel et al., 2021).

6. Discussion

6.1. Age, biostratigraphic correlation, and paleoclimate

Of the 26 palynotaxa (23 microspores, three megaspores, Fig. 2), 21 species are geographically widespread, whereas the remaining taxa are currently considered endemic to Laurussia (*Camptozonotriletes aliquantus, Camptozonotriletes mcgregorii, Chelinospora perforata, Perotrilites conatus, Punctatisporites scabratus*). Among the cosmopolitan species, the early Givetian to Famennian *Geminospora lemurata* is common to abundant in all four samples.

Our initial estimate of the age of the Maywood's assemblage, as presented in Zatoń et al. (2021), was middle Givetian, which was based in part on the presence of the microspore *Samarisporites triangulatus* (documented in sample CICYTTP-Pl 2606). However, we are herein modifying that age based on additional sample material, which yielded *Contagisporites optivus* in all four samples (Fig. 2). The presence of both *C. optivus* and *S. triangulatus* are diagnostic of the following zones (Fig. 3): 1) *Samarisporites triangulatus–Cymbosporites catillus* Zone of the middle–upper Givetian of Saudi Arabia (Steemans et al., 2011; Breuer and Steemans, 2013), 2) *Contagisporites optivus–S. triangulatus* (OT) of North America (Richardson and McGregor, 1986), 3) *S. triangulatus–Ancyrospora ancyrea* (TA) of Europe (Streel et al., 1987), 4) *S. triangulatus–Corystisporites serratus* Subzone of Eastern Europe (Avkhimovitch et al., 1993; see also Turnau, 2014), and 5) *S. triangulatus* Interval Zone (Trg) of Brazil (Melo and Loboziak, 2003; Breuer and Grahn, 2011; Breuer and Steemans, 2013, and references therein), which is also recognized in Argentina and Bolivia (di Pasquo et al., 2009, 2015; Noetinger and di Pasquo, 2011; Noetinger et al., 2018, and references therein).

Most importantly, these zones are correlative with the East European *Contagisporites optivus–Spelaeotriletes krestovnikovii* (OK) palynozone (Fig. 3), which ranges from upper Givetian to lowermost Frasnian (Avkhimovitch et al., 1993; Turnau and Racki, 1999). The Maywood assemblage is nearly identical to the Berstane Member of the Eday Formation from Orkney (Orcadian Basin) in the United Kingdom, which is assigned to the same palynozone and is dominated by *Geminospora lemurata* and the associated megaspore *Contagisporites optivus*. Marshall et al. (2011) assigned those strata to the upper Givetian, which supports a more restricted upper Givetian age for the Maywood strata at Cottonwood Canyon (Fig. 3).

Phosphatic fish fossils in the Maywood Formation at our Cottonwood Canyon locality may also have bearing on the age of the strata. Sandberg (1963) noted the following phosphatic fauna from the Maywood: *Bothriolepis* cf. *B. coloradensis*, palaeoniscoid teeth *Rhadinichthys* sp., coccosteid plates, heterostracan carapaces, and the crossopterygian *Holoptychius* cf. *H. giganteus* Eastman. The heterostracan material is particularly significant, as all taxa in the group, except psammosteids, went extinct at the end of the Givetian (Young, 2003; Randle and Sansom, 2017), and the only known psammosteids in North America are from the Canadian Arctic (Elliott et al., 2004). However, the fish fossils in Sandberg (1963) were not photographed and described formally, and no heterostracan remains have been found among numerous SEM photographs, made by the authors, of fish remains from the Cottonwood

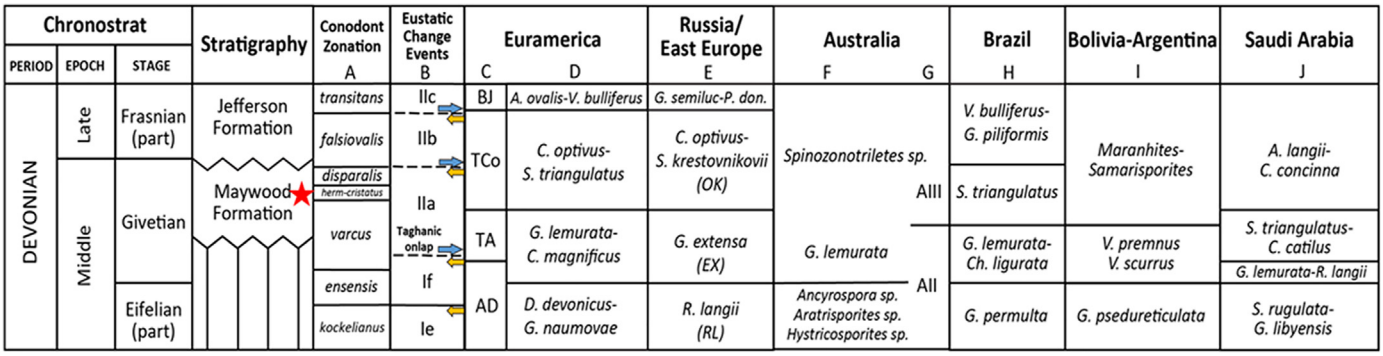

Fig. 3. Correlation chart of the Cottonwood Canyon Maywood assemblages (red star) and palynozones or assemblages of the Middle to early Late Devonian. References: A: standard conodont zones of Devonian (part); B: eustatic events with orange arrows (sea level fall) and light blue arrows (sea level rise), modified from Johnson and Sandberg (1989), Sandberg et al. (2002), Grader et al. (2016); C: Streel et al. (1987); D: Richardson and McGregor (1986); E: Avkhimovitch et al. (1993); F: Playford (1985, 1991), Young (1996); G: Hashemi and Playford (2005); H: Melo and Loboziak (2003); I: Limachi et al. (1996), see also di Pasquo et al. (2009), Noetinger and di Pasquo (2011); J: Breuer and Steemans (2013). Abbreviations: (Euramerica) *BJ –V. bulliferus-C. jekhowskyi, TCo – S. triangulatus-C. concinna, TA – S. triangulatus-A. ancyrea, AD – A. acanthomammillatus-D. devonicus*, (Russia) *G. semilucensis-P. donensis.* (For interpretation of the references to color in this figure legend, the reader is referred to the web version of this article.)

Canyon Maywood outcrops (viewed by David Elliot, Susan Turner, and Michael Coates, pers. comm., 2021).

On the other hand, *Rhabdosporites streelii* and *Dictyotriletes hemeri*, both present in the samples, are in fact restricted to the Givetian, whereas other taxa are most commonly documented in strata of this age (e.g., *Aneurospora goensis*, *Archaeozonotriletes variabilis, Biharisporites parviornatus*, *Cymbosporites catillus*, *Densosporites devonicus*, *Geminospora punctata, Grandispora gabesensis*, *Perotrilites conatus, Retusotriletes dubiosus*, *Retusotriletes distinctus, Scylaspora rugulata*).

Two taxa of little biostratigraphic utility in our samples are (1) *Musivum gradzinskii* Wood and Turnau (2001), which has been described from the upper Givetian of Poland and later documented from the Emsian to Frasnian of Poland, China, and Saudi Arabia (see Marshall et al., 2017); and (2) *Punctatisporites scabratus*, which McGregor (1960) recorded in Frasnian deposits. The evidence above reinforces a latest Givetian age for the Maywood Formation.

The middle to upper Givetian was a time of widespread sea level rise called the "Taghanic transgression/onlap", as first recognized in North America (Johnson, 1970; Johnson et al., 1985; Sandberg et al., 1988, 1997; Johnson and Sandberg, 1989). Later, the term "Taghanic crisis" was used to represent a series of sea-level changes and associated faunal/floral extinctions that took place entirely within the late middle to upper *varcus* (conodont) Zone (Algeo and Scheckler, 1998; Aboussalam, 2003; Aboussalam and Becker, 2011; Marshall et al., 2011; Turnau, 2014). The crisis, which is well recorded in Poland (Turnau and Racki, 1999; Turnau, 2011, cited by Turnau, 2014), included a reduction in the abundance of aneurophytes (e.g., *R. langii*) and an increase in archaeopterids progymnosperm (e.g., *G. lemurata* and *C. optivus*). During this time, marine regressions were associated with warming pulses and arid conditions (Aboussalam and Becker, 2011; Marshall et al., 2011), as suggested by brachiopod and conodont $\delta^{18}O$ isotope data (Joachimski et al., 2004; van Geldern et al., 2006), and migration of warm-water species into high latitudes (Leanza, 1968; House, 1978; Boucot and Theron, 2001). During these climatic changes plant diversity dropped, but archaeopterids and aneurophytes that were far from shore were better adapted and had higher survival rates (Marshall et al., 2011; Turnau, 2014; Stein et al., 2020).

Our designation of the Maywood to the *C. optivus/S. triangulatus* Zone would indicate assignment to uppermost *varcus* to uppermost *falsiovalis* conodont zones. However, if correlation to the Bernstane Member of the Eday Formation is correct, then the Maywood would be *hermanni* Zone or younger (i.e., postdate the *varcus*) (Marshall et al., 2011). Thus, the Maywood palynoflora is a record of the latest Taghanic crisis or earliest post-Taghanic interval (Fig. 3).

6.2. Floral composition and environments of deposition

The Givetian Stage was an important time in the evolution of plants in general throughout the world, and specifically in the evolution of heterosporous reproduction, including an increase in size of megaspores (e.g., Steemans et al., 2012). The sizes of the megaspores in our collections range from 180 μm up to 600 μm, depending on the megaspore species (Fig. 2). This range is comparable to that of the Givetian assemblage from Libya, which Steemans et al. (2011) considered as one of the richest from the Middle Devonian in Gondwana (see also de Ville de Goyet et al., 2007). Dilcher et al. (1992) noted the difficulty in eolian transport of megaspores, and especially those bearing spinate and bifurcate processes of the genera *Ancyrospora* and *Hystrichosporites*, and concluded that many Devonian heterosporous plants were probably adaptated to aquatic environments and/or to climatic factors (de Ville de Goyet et al., 2007). Those genera of megaspores are absent in our samples. Instead, the most abundant well-preserved microspores namely *Geminospora* and *Aneurospora*, and megaspores *Biharisporites* and *Contagisporites* (Fig. 2), larger than 300 μm documented in the four samples, include two forms with a tree-like habit, and these are assigned to Aneurophytales and Archaeopteridales (Progymnosperm). We have also identified in our samples the presence of fusiform sporangia and other plant fragments assigned herein to *Archaeopteris* sp. (Plate II). These plants are known to have lived in proximal fluvio-lacustrine settings of floodplain and paralic environments of internal basins (see Streel and Scheckler, 1990). Other plants that colonized the terrestrial landscape near the Maywood valley include the herbaceous lycopsid Selaginellales (*Camptozonotriletes*, *Densosporites*), the shrubby lycopods Protolepidodendrales (*Acinosporites*) and Drepanophycales (*Retusotriletes, Granulatisporites*), and allies of *Barinophytopsida* and primitive ferns (*Cymbosporites, Dibolisporites, Punctatisporites, Retusotriletes, Scylaspora*). Hence, we confirm that the terrestrial, freshwater Maywood flora was transported a short distance by fluvial currents into the Maywood valley. We do not discard the influence of wind dispersal of mega-microspores from non-laminated fertile leaves of archaeopteridaleans as suggested by Fairon-Demaret et al. (2001) for *A. roemeriana* trees.

The palynofacies features show: 1) a predominance of well-preserved terrestrial microspores, megaspores, and tetrads; 2) a low frequency of terrestrial debris (mostly tracheids); 3) an abundance of fine granular-fibrous and lumpy AOM types with orange fluorescence, indicating preferential contributions of organic matter decomposition from algal sources and other aquatic fossils (e.g., tentaculitoid tubeworms, fishes); 4) a scarce and poorly diversified group of marine–brackish prasinophytes; and 5) the presence of minor pyrite in one sample (Fig. 2, Plates I–VIII). The prasinophytes and pyrite, the latter of which is diagnostic of diagenesis in dysaerobic to anoxic

conditions in surficial sediment, are consistent with at least temporary brackish to marine water influence, which would have been a source of sulfur ions for the pyrite. Fossils diagnostic of fully marine conditions, such as conodonts and ammonoids were not found in our samples or previously by Zatoń et al. (2021).

Our palynoassemblages are associated with grainstone beds dominated by a monospecific assemblage of microconchid tubeworms *Aculeiconchus sandbergi*, described by Zatoń et al. (2021). This new species developed unique hollow spine-like structures of various lengths on the tube underside, likely for fixation to flexible substrates, such as algal thalli, similarly to tubular extensions in fossil and modern cyclostome bryozoans. The basal spines of *Aculeiconchus* were possibly attached to non-biomineralized algae that degraded quickly after death, leaving the microconchids scattered loosely within the sediment (Plate I). The fossils represent at least parautochthonous assemblages, as they are well-preserved, and the spines are often intact, thus reinforcing the environmental interpretation above. The lack of other benthic fossils, and especially other encrusting organisms, clearly indicate that the *Aculeiconchus* microconchids, similarly to many other microconchid species from different stratigraphic intervals (e.g., Zatoń et al., 2012), were opportunistic taxa that colonized the salinity-stressed Maywood paleovalleys. Fluctuations in salinity were likely, generated by mixing of marine and freshwater input within estuarine channels developed along the paleoshorelines of the Maywood Sea (Sandberg, 1963; Mikesh, 1965). The microconchids could have fed on suspended organic matter and would have co-existed with a diverse suite of fish fossils (e.g., Sandberg, 1963; Sandberg et al., 1988; Zatoń et al., 2021, and references herein) in these stressed ecological niches, all of which could have helped to preserve spores and other organic matter in shells (microconchids, Plate I) and pellets (fish), increasing their distribution into the environments of deposition.

6.3. Paleobiology and paleobiogeography

The global degree of provincialism for both fauna and flora was high through the Early Devonian and reached its maximum in the early Middle Devonian Eifelian Stage (e.g., Johnson, 1970; Klapper and Johnson, 1980; Allen and Dineley, 1988; Breuer et al., 2009), in part due to the presence of the Rheic Ocean, which existed between Laurussia and western Gondwana from the Ordovician to Carboniferous (Allen and Dineley, 1988; Breuer et al., 2009; di Pasquo et al., 2009; Nance et al., 2012; Golonka, 2020). An interval of more cosmopolitanism took place during the latest Eifelian to Frasnian (Johnson, 1970; Klapper and Johnson, 1980), in which marine faunas, e.g., *Bothriolepis*, developed in eastern Gondwana and spread elsewhere (see Young, 2003; Stock, 2005; Young and Lu, 2020). After the middle *varcus* Zone of the middle Givetian, the rate of cosmopolitanism then increased through the Late Devonian, particularly among benthic fauna (e.g., brachiopods, corals) and conodonts (Johnson, 1970; Klapper and Johnson, 1980; Ziegler and Lane, 1987; Johnson and Sandberg, 1989; Sandberg et al., 2002; Baird et al., 2012). Also, the antiarch placoderm *Bothriolepis* was suggested to have migrated from Gondwana to western Laurussia (Young, 2003). During this time, terrestrial environments were mainly colonized by progymnosperms and lycopsids and their related spores (e.g., McGregor and Playford, 1992; Marshall, 1996b; Algeo and Scheckler, 1998; Meyer-Berthaud et al., 2003, 2016; Cornet et al., 2012; Stein et al., 2020) (Fig. 4).

In terms of spore diversity, there was a reduction in the middle to late Givetian (middle *varcus* to *hermanni* zones (Fig. 3) driven by episodic aridity, as recorded in different sections throughout the world (Baird and Brett, 2008; Aboussalam and Becker, 2011; Marshall et al., 2011). The Maywood paleoflora includes such a cosmopolitan palynologic assemblage, typical of western North America, with spores of late Givetian archaeopteridaleans (Fig. 4), although it also includes certain endemic spore taxa mainly of lycopsid affinity. We are unable to identify a diversity reduction of spore in our relatively thin succession of the Maywood Formation. However, given the age (Fig. 3) and correlation proposed herein of the Maywood palynoflora with that of the Berstane Member of the uppermost Eday Formation (Marshall et al., 2011), our deposits likely postdated the major diversity reduction. The reduction in spore diversity is most pronounced in European successions (Brice et al., 1979; Turnau and Racki, 1999; Marshall et al., 2011; Turnau, 2014), e.g., the lower Eday Formation (Marshall et al., 2011), and less

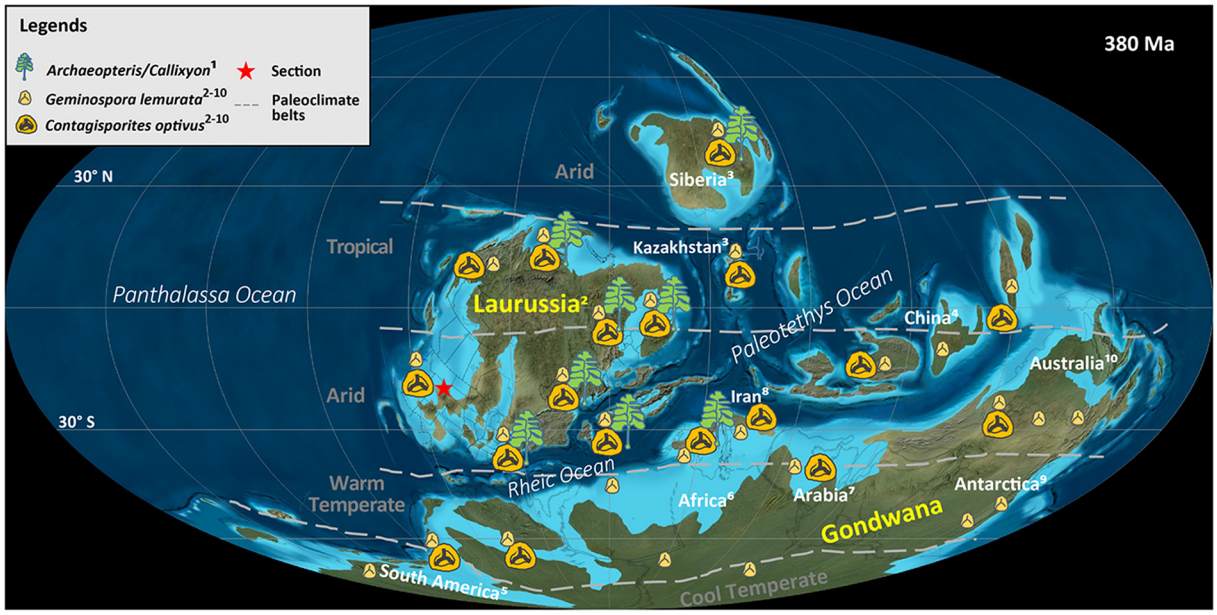

Fig. 4. Givetian occurrences of *Archaeopteris* and *Callixylon* fossil plants, and Archaeopteridales based on records of *Geminospora lemurata* and *Contagisporites optivus*. Mollweide basemap after Blakey (2016), and paleoclimatic belts after Scotese (2013). (1) It represents distribution of *Archaeopteris/Callixyon*, and (2)–(10) are for spores. (1) Cornet et al. (2012); also see, Anderson et al. (1995), Taylor et al. (2009), Stein et al. (2020), Davies et al. (2021). (2) Laurussia: Allen (1965), Whiteley (1980), Richardson and McGregor (1986), Marshall (1996a, 1996b, 2000), Marshall et al. (1996, 2011), Turnau and Racki (1999), Steemans et al. (2011), Turnau (2014), Berry and Marshall (2015), Streel et al. (2021). (3) Siberia and Kazakhstan: Avkhimovitch et al. (1993), Tel'nova (2008), Gutak et al. (2011). (4) China: Gao (1981), Shen et al. (2020); (5) South America: Ottone (1996), di Pasquo et al. (2009, 2015), Noetinger and di Pasquo (2011), Grahn et al. (2013), Noetinger (2015), di Pasquo et al. (2015), Noetinger et al. (2018). (6) Africa: Loboziak and Streel (1989), Marshall (1996b). (7) Arabia: Breuer and Steemans (2013). (8) Iran: Ghavidel-Syooki (2003). (9) Antarctica: Marshall (1996b). (10) Australia: Playford (1983), Grey (1991), Marshall (1996b).

abrupt in successions in Laurentia (see Turnau, 2014). There was also a reduction in the abundance of Aneurophytes (e.g., *R. langii*) and an increase in archaeopterids progymnosperm (e.g., *G. lemurata* and *C. optivus*). The latter formed true tree canopies for the first time (Berry and Fairon-Demaret, 2001), which altered the habitats of the undergrowth and produced forest litter (Meyer-Berthaud et al., 1999) that helped retain moisture (Algeo et al., 2001). These changes, along with such adaptations as deep penetrating and basal spreading roots, allowed progymnosperms to adapt to more xerophylous soils and tolerate arid conditions (see Turnau, 2014; Stein et al., 2020; Davies et al., 2021). During Givetian *Archaeopteris* is rather restricted to Laurussia (North America and western and Eastern Europe) and Siberia (Fig. 4), whereas it expanded to northern Gondwana (Venezuela, Morocco) and China in the Frasnian (Cornet et al., 2012). Furthermore, in Famennian this taxon is extended to Australia (Eastern Gondwana) and also in southern Africa, demostrating a great capacity to migrate and adapt to different conditions worldwide (Anderson et al., 1995; Cressler III, 2006; Guo and Wang, 2011; Gutak et al., 2011; Orlova et al., 2016; Guo et al., 2019; Stein et al., 2020; Davies et al., 2021).

These paleobotanical trends were driven by a decrease in latitudinal climatic gradients due in part to the narrowing of the warm Rheic Ocean (Scotese et al., 1999; di Pasquo et al., 2009), which sat at low latitudes between the Gondwana and Laurussia continents (Marshall et al., 2007; Steemans et al., 2011; Nance et al., 2012). The reduction of this paleogeographic barrier resulted in greater floral dispersal, as indicated by the presence of similar Givetian microspore and megaspore taxa that are mostly represented by *Geminospora lemurata* and *Contagisporites optivus* and fossil plants of *Archaeopteris* and *Callixylon* (Fig. 4). This change in paleogeography caused a brief, rapid rise in temperature during the late Givetian (W19, Givetian Thermal Maximum, GAT = 21.2 °C; Scotese et al., 2021), which was associated with an increase in aridity, as mentioned above.

7. Conclusions

The Middle Devonian Maywood Formation at Cottonwood Canyon in Wyoming, USA, contains 26 palynotaxa, of which 21 species have wide paleogeographical distribution and five species are considered endemic to Laurussia. The previous middle Givetian age of the Maywood Formation is now revised and established as late Givetian based on the presence of such microspore species as *Samarisporites triangulatus* and *Contagisporites optivus*, which are indicative for the *C. optivus*/*S. triangulatus* palynozone, as well as others that are restricted to the Late Givetian. The palynoflora investigated correlates with the *hermanni* or younger (postdate the *varcus*) conodont Zone, and thus they record the latest Taghanic crisis or earliest post-Taghanic interval. The crisis was related to sea-level changes and associated fauna and flora extinctions, both of which have been linked to climatic changes.

The Maywood palynoflora is dominated by microspores and megaspores (*Geminospora*, *Aneurospora*, *Biharisporites* and *Contagisporites*), including progymnosperms that have tree-like habit (Aneurophytales and Archaeopteridales) characteristic of proximal fluvio-lacustrine settings of floodplain and paralic environments of internal basins. Additionally, there are spores of the herbaceous lycopsid Selaginellales (*Camptozonotriletes*, *Densosporites*), shrubby lycopods Protolepidodendrales (*Acinosporites*) and Drepanophycales (*Retusotriletes*, *Granulatisporites*), and primitive ferns (*Cymbosporites*, *Dibolisporites*, *Punctatisporites*, *Retusotriletes*, *Scylaspora*), all of which lived in the terrestrial landscape near the Maywood valley.

The association of such terrestrial palynoflora with (1) a low diversity marine-brackish algal taxa (*Dictyotidium*, *Quadrisporites*); (2) monospecific microconchid tubeworms that colonized non-biomineralized, flexible algal thali, and (3) a lack of other marine fossils, indicates that the habitat of the Maywood paleovalleys was influenced by fluctuations of salinity due to mixing of marine and freshwater input within estuarine channels developed along the paleoshorelines of the Maywood Sea.

Fundings

CONICET PIP 0812 (2015–2017).

Declaration of Competing Interest

Conflict of interest with John Marshall from National Oceanography Centre, Southampton.

Acknowledgments

The authors are grateful to the institutions that allowed carrying out this work on their respective laboratories. We thank Charles Sandberg for considerable help with locations, stratigraphy, and overall understanding of the Maywood Formation and associated units. We also thank David Elliot, Susan Turner, and Michael Coates for examination of images of fish fossils. To Leonardo Silvestri for processing the palynologic samples and Jose Vilá for his assistance taking SEM pictures at the CICYTTP (CONICET-ER-UADER) in Diamante, Argentina. This research was funded by CONICET PIP 0812 (2015-2017).

References

Aboussalam, Z.S., 2003. Das «Taghanic-Event» im höheren Mittel-Devon von West-Europa und Marokko. Münstersch. Forsch. Geol. Paläontol. 97, 1–332.
Aboussalam, Z.S., Becker, R.T., 2011. The global Taghanic Biocrisis (Givetian) in the eastern Anti-Atlas, Morocco. Palaeogeogr. Palaeoclimatol. Palaeoecol. 304, 136–164.
Algeo, T.J., Scheckler, S.E., 1998. Terrestrial-marine teleconnections in the Devonian: links between the evolution of land plants, weathering processes, and marine anoxic events. Philos. Trans. R. Soc. Lond. B 353, 113–130. https://doi.org/10.1098/rstb.1998.0195.
Algeo, T.J., Scheckler, S.E., Maynard, J.B., 2001. Effects of early vascular land plants on weathering processes and global chemical fl uxes during the Middle and late Devonian. In: Gensel, P.G., Edwards, D. (Eds.), Plants Invade the Land: Evolutionary and Environmental Perspectives. Columbia University Press, New York, pp. 83–102.
Allen, K.C., 1965. Lower to Middle Devonian spores of North and Central Vestspitsbergen. Palaeontology 8, 687–748.
Allen, K.C., 1982. *Samarisporites triangulatus* Allen 1965, an important Devonian miospore, and its synonymous species. Pollen Spores 24, 157–166.
Allen, K.C., Dineley, D.L., 1988. Mid-Devonian to mid-Permian floral and faunal regions and provinces. Geol. Soc. Lond., Spec. Publ. 38, 531–548.
Anderson, H.M., Hiller, N., Gess, R.W., 1995. *Archaeopteris* (Progymnospermopsida) from the Devonian of southern Africa. Bot. J. Linn. Soc. 117, 305–320.
Avkhimovitch, V.I., Tchibrikova, E.V., Obukhovskaya, T.G., Nazarenko, A.M., Umnova, V.T., Raskatova, L.G., Mantsurova, V.N., Loboziak, S., Streel, M., 1993. Middle and Upper Devonian miospore zonation of Eastern Europe. Bull. Centres Recher. Explorat. Prod. Elf Aquit. 17, 79–147.
Azcuy, C.L., di Pasquo, M.M., 2005. Early Carboniferous palynoflora from the Ambo Formation, Pongo de Mainique, Peru. Rev. Palaeobot. Palynol. 134 (3/4), 153–184.
Baird, G.C., Brett, C.E., 2008. Late Givetian Taghanic bioevents in New York State: new discoveries and questions. Bull. Geosci. 83, 357–370.
Baird, G.C., Zambito, J.J., Bret, C.E., 2012. Genesis of unusual lithologies associated with the late Middle Devonian Taghanic biocrisis in the type Taghanic succession of New York State and Pennsylvania. Palaeogeogr. Palaeoclimatol. Palaeoecol. 367–368, 121–136.
Balme, B.E., 1962. Upper Devonian (Frasnian) spores from the Carnarvon Basin, Western Australia. The Palaeobotanist 9, 1–10.
Balme, B.E., 1988. Miospores from Late Devonian (early Frasnian) strata, Carnarvon Basin, Western Australia. Palaeöntogr. Abt B 209, 109–166.
Balme, B.E., 1995. Fossil *in situ* spores and pollen grains: an annotated catalogue. Rev. Palaeobot. Palynol. 87, 81–323.
Beck, C.B., 1971. On the anatomy and morphology of lateral branch system of *Archaeopteris*. Am. J. Bot. 58, 758–784.
Berry, W., 1937. Spores from the Pennington Coal, Rhea County, Tennessee. Am. Midl. Nat. 150–160.
Berry, C.M., Fairon-Demaret, M., 2001. The Middle Devonian flora revisited. In: Gensel, P.G., Edwards, D. (Eds.), Plants Invade the Land. Columbia Univ. Press, N.Y, pp. 83–102.
Berry, C.M., Marshall, J.E.A., 2015. Lycopsid forests in the early Late Devonian paleoequatorial zone of Svalbard. Geology 43 (12), 1043–1046. https://doi.org/10.1130/G37000.1.
Blakey, R., 2016. Global Paleogeography and Tectonics in Deep Time. Colorado Plateau Geosystems Inc. Link to Deep Time Maps™ . https://deeptimemaps.com/.
Boucot, A.J., Theron, J.N., 2001. First *Rhipidothyris* (Brachiopoda) from South Africa: biostratigraphic, palaeoecological and biogeographical significance. J. Czech Geol. Soc. 46 (3), 155–160.

Braman, D.R., Hills, L.V., 1992. Upper Devonian and Lower Carboniferous miospores, western District of Mackenzie and Yukon Territory, Canada. Palaeöntogr. Can. 8, 1–97.
Breuer, P., Grahn, Y., 2011. Middle Devonian spore stratigraphy in the eastern outcrop belt of the Parnaíba Basin, northeastern Brazil. Rev. Esp. Micropaleontol. 43 (1–2), 19–38.
Breuer, P., Steemans, P., 2013. Devonian spore assemblages from Northwestern Gondwana: Taxonomy and Biostratigraphy. Special Papers in Palaeontology. 89. The Palaeontological Association, London, p. 163.
Breuer, P., Al-Ghazi, A., Al-Ruwaili, M., Higgs, K.T., Steemans, P., Wellman, C.H., 2007. Early to Middle Devonian miospores from northern Saudi Arabia. Rev. Micropaléontologie 50, 27–57.
Breuer, P., Steemans, P., di Pasquo, M., 2009. Palaeopytogeography of Devonian miospore assemblages. The CIMP Faro'09, II Joint Meeting of Spores/Pollen and Acritarch CIMP Subcommissions (Faro, Portugal, 20-24th September 2009), CIMA (University of the Algarve), Abstracts and short papers, pp. 17–22.
Brice, D., Bultynck, P., Deunff, J., Loboziak, S., Streel, M., 1979. Données biostratigraphiques nouvelles sur le Givétien et le Frasnien de Ferques (Boulonnais, France). Ann. Soc. Géol. Nord. 98, 325–344.
Brugger, J., Hofmann, M., Petri, S., Feulner, G., 2019. On the sensitivity of the Devonian climate to continental configuration, vegetation cover, orbital configuration, CO_2 concentration, and insolation. Paleoceanogr. Paleoclimatol. 34, 1375–1398. https://doi.org/10.1029/2019PA003562.
Buggisch, W., Joachimski, M.M., 2006. Carbon isotope stratigraphy of the Devonian of Central and Southern Europe. Palaeogeogr. Palaeoclimatol. Palaeoecol 240, 68–88.
Burgess, N.D., Richardson, J.B., 1995. Late Wenlock to early Pridoli cryptospores and spores from south and southwest Wales Great Britain. Palaeöntogr. Abt. B 236, 1–44.
Burjack, M.I.A., Loboziak, S., Streel, M., 1987. Some new data on the Devonian miospores of the Paraná Basin (Brazil). Sci. Géol. Bull. 40, 381–391.
Carluccio, L.M., Hueber, F.M., Banks, H.P., 1966. *Archaeopteris macilenta*, anatomy and morphology of its frond. Am. J. Bot. 53, 719–730.
Caruso, J.A., Tomescu, A.M.F., 2012. Microconchid encrusters colonizing land plants: the earliest north American record from the Early Devonian of Wyoming, USA. Lethaia 45, 490–494.
Chaloner, W.G., 1959. Devonian megaspores from Arctic Canada. Palaeontology 1, 321–332.
Chi, B., Hills, L., 1976. Biostratigraphy and taxonomy of Devonian megaspores, Arctic Canada. Bull. Can. Petrol. 24 (4), 641–817.
Chitaley, McGregor, D.C., 1988. *Bisporangiostrobus harrisi* gen. et sp. nov., an eligulate lycopsid cone with *Duosporites* megaspores and *Geminospora* microspores from the Upper Devonian of Pennsylvania, U.S.A. Palaeöntographica, Abteilung B 210, 127-149. Palaeöntographica, Abteilung B 210, 127–149.
Cohen, K.M., Harper, D.A.T., Gibbard, P.L., 2020. ICS International Chronostratigraphic Chart 2020/03. International Commission on Stratigraphy, IUGS. https://stratigraphy.org/ICSchart/ChronostratChart2020-03.pdf/ (accessed 11 January 2021).
Cornet, L., Gerrienne, P., Meyer-Berthaud, B., Prestianni, C.A., 2012. Middle Devonian *Callixylon* (Archaeopteridales) from Ronquières, Belgium. Rev. Palaeobot. Palynol. 183, 1–8.
Couper, R.A., 1953. Upper Mesozoic and Cainozoic spores and pollen grains from New Zealand. New Zeal. Geol. Surv. Paleontol. Bull. 22, 5–77.
Cressler III, W.L., 2006. Plant paleoecology of the Late Devonian Red Hill locality, north-central Pennsylvania, an *Archaeopteris* dominated wetland plant community and early tetrapod site. In: DiMichele, W.A., Greb, S. (Eds.), Wetlands Through Time. Geological Society of America, Special Paper 399, pp. 79–102.
Davies, N.S., Berry, C.M., Marshal, J.E.A., Wellman, C.H., Lindemann, F., 2021. The Devonian landscape factory: plant–sediment interactions in the Old Red Sandstone of Svalbard and the rise of vegetation as a biogeomorphic agent. J. Geol. Soc. Lond. https://doi.org/10.1144/jgs2020-225.
de Ville de Goyet, F., Breuer, P., Gerrienne, P., Prestianni, C., Streel, M., Steemans, P., 2007. Middle Devonian (Givetian) megaspores from Belgium (Ronquières) and Libya (A1-69 borehole). In: Steemans, P., Javaux, E.J. (Eds.), Recent Advances in Palynology: Carnets de Géologie/Notebooks in Geology, Brest, pp. 68–73.
di Pasquo, M.M., 2007. Asociaciones palinológicas en las formaciones Los Monos (Devónico) e Itacua (Carbonífero Inferior) en Balapuca (cuenca Tarija), sur de Bolivia. Parte 1. Formación Los Monos. Rev. Geol. Chile 34 (1), 97–137.
di Pasquo, M.M., Silvestri, L., 2014. Las colecciones de Palinología y Paleobotánica del Laboratorio de Palinoestratigrafía y Paleobotánica del Centro de Investigaciones Científicas y Transferencia de Tecnología a la Producción (CICYTTP), Entre Ríos, Argentina. Contribuição à RESCEPP "Rede Sul-americana de Coleções e Ensino em Paleobotânica e Palinologia". Bol. Asoc. Latinoam. Paleobot. Palinol. 14, 39–47.
di Pasquo, M., Vilá, J., 2019. SEM Observation of Non-Metallized Samples in Paleopalynology. Microscopy & MicroAnalysis Journal 26, 149–150. https://doi.org/10.1017/S1551929519000798.
di Pasquo, M., Amenábar, C.R., Noetinger, S., 2009. Middle Devonian microfloras and megafloras from western Argentina and southern Bolivia. Its importance in the palaeobiogeographical and palaeoclimatical evolution of western Gondwana. In: Königshof, P. (Ed.), Devonian Change: Case Studies in Palaeogeography and Palaeoecology. Special Publications314. The Geological Society, London, pp. 193–213.
di Pasquo, M., Noetinger, S., Isaacson, P., Grader, G., Starck, D., Morel, E., Anderson Folnagy, H., 2015. Mid-Late Devonian assemblages of herbaceous lycophytes from northern Argentina and Bolivia: age assessment with palynomorphs and invertebrates and paleobiogeographic importance. J. S. Am. Earth Sci. 63, 70–83. https://doi.org/10.1016/j.jsames.2015.06.010.
Dilcher, D.L., Kar, R.K., Dettmann, M.E., 1992. The functional biology of Devonian spores with bifurcate processes - a hypothesis. Palaeobotanist 41, 67–74.
Dorobek, S.L., Reid, S.K., Elrick, M., 1991. Antler foreland stratigraphy of Montana and Idaho: The stratigraphic record of eustatic fluctuations and episodic tectonic events. In: Cooper, J.D., Stevens, C.H. (Eds.), Paleozoic Paleogeography of the Western United States II. Pacific Section, SEPM, Bookvol. 67, pp. 487–507.
Elliot, D.K., Ilyes, R.R., 1996. Lower Devonian vertebrate biostratigraphy of the western United States. Mod. Geol. 20, 253–262.
Elliot, D.K., Johnson, H.G., 1997. Use of vertebrates to solve biostratigraphic problems: examples from the Lower and Middle Devonian of western North America. In: Klapper, G., Murphy, M.A., Talent, J.A. (Eds.), Paleozoic Sequence Stratigraphy, Biostratigraphy, and Biogeography, Studies in Honor of J. Granville ("Jess"). Geological Society of America Special Paperv. 321, pp. 179–188.
Elliott, D.K., Mark-Kurik, E.L.G.A., Daeschler, E.B., 2004. A revision of *Obruchevia* (Psammosteida: Heterostraci) and a description of a new obrucheviid from the late Devonian of the Canadian Arctic. Acta Univ. Latv. 679, 22–45.
Evans, P.R., 1970. Revision of the miospore genera *Perotrilites*, Erdtmann ex Couper, 1953 and *Diaphanospora* Balme and Hassell, 1962. Bureau Miner. Resour. Geol. Geophys. Bull. 116, 65–71.
Fairon-Demaret, M., Leponce, I., Streel, M., 2001. *Archaeopteris* from the Upper Famennian of Belgium: heterospory, nomenclature and paleobiogeography. Rev. Paleobot. Palynol. 115, 79–97.
Fiorillo, A.R., 2000. The ancient environment of the Beartooth Butte Formation (Devonian) in Wyoming and Montana: Combining paleontological inquiry with Federal Management needs. Proceedings of USDA Forest Service, RMRS-P-15. 3, pp. 160–167.
Gao, L., 1981. Devonian spore assemblages of China. In: Owens, B., Visscher, H. (Eds.), Late Palaeozoic and Early Mesozoic Stratigraphic Palynology. Review of Palaeobotany and Palynologyvol. 34, pp. 11–23.
Ghavidel-Syooki, M., 2003. Palynostratigraphy of Devonian sediments in the Zagros Basin, southern Iran. Rev. Palaeobot. Palynol. 127, 241–268.
Goddéris, Y., Joachimski, M.M., 2004. Global change in the Late Devonian: modelling the Frasnian–Famennian short-term carbón isotope excursions. Palaeogeogr. Palaeoclimatol. Palaeoecol 202, 309–329.
Golonka, J., 2020. Late Devonian paleogeography in the framework of global plate tectonics. Global and Planetary Change 186, 103129.
Grader, G.W., Dehler, C.M., 1999. Devonian stratigraphy in east-central Idaho: New perspectives from the Lemhi Range and Bayhorse area. In: Hughes, S.S., Thackray, G.D. (Eds.), Guidebook to the Geology of Eastern Idaho, Idaho Museum of Natural History, Pocatello, pp. 31–56.
Grader, G.W., Isaacson, P.E., Doughty, P.T., Pope, M.C., DeSantis, M.K., 2016. Idaho Lost River Shelf to Montana Craton: North American Late Devonian stratigraphy, surfaces, and intrashelf basin. In: Playton, E., Kerans, C., Eissenberger, J.A.W. (Eds.), New Advances in Devonian Carbonates: Outcrop analogs, reservoirs, and chronostratigraphy. SEPM (Society for Sedimentary Geology) Special Publication No. 107, pp. 347–379.
Grahn, Y., Mauller, P.M., Bergamaschi, S., Bosetti, E.P., 2013. Palynology and sequence stratigraphy of three Devonian rock units in the Apucarana Sub-basin (Paraná Basin, South Brazil): additional data and correlation. Rev. Palaeobot. Palynol. 198, 27–44.
Grey, K., 1991. A mid-Givetian spore age for the onset of reef development on the Lennard Shelf, Canning Basin, Western Australia. Rev. Palaeobot. Palynol. 68, 37–48.
Guo, Y., Wang, D.-M., 2009. *Archaeopteris halliana* from the Late Devonian of Anhui Province, China. Acta Geol. Sin. 83, 479–491.
Guo, Y., Wang, D.-M., 2011. Anatomical reinvestigation of *Archaeopteris macilenta* from the Upper Devonian (Frasnian) of South China. J. Syst. Evol. 49 (6), 590–597.
Guo, X., Xu, H., Zhu, X., Pang, Y., Zhang, X., Lu, H., 2019. Discovery of Late Devonian plants from the southern Yellow Sea borehole of China and its palaeogeographical implications. Palaeogeogr. Palaeoclimatol. Palaeoecol. 531, 108444.
Gutak, J.M., Antonova, V.A., Ruban, D.A., 2011. Diversity and richness of the Devonian terrestrial plants in the Southeastern Mountainous Altay (Southern Siberia): Regional versus global patterns. Palaeogeogr. Palaeoclimatol. Palaeoecol. 299, 240–249.
Hartkopf-Fröder, C., Streel, M., 1994. Late Famennian miospore assemblages from the Bergisch Gladbach-Paffrath Syncline, Rhenish Slate Mountains, Germany. Ann. Soc. Geol. Belg. 116, 333–357.
Hashemi, H., Playford, G., 2005. Devonian spore assemblages of the Adavale Basin, Queensland (Australia): descriptive systematics and stratigraphic significance. Rev. Esp. Micropaleontol. 37, 317–417.
Hoffmeister, W.S., Staplin, F.L., Malloy, R.E., 1955. Mississippian plant spores from Hardinsburg Formation of Illinois and Kentuky. J. Paleontol. 29, 372–399.
Holland, S.M., Patzkowsky, M.E., 2009. The stratigraphic distribution of fossils in a Tropical Carbonate Succession: Ordovician Bighorn Dolomite, Wyoming, USA. Palaios 24 (5/6), 303–317. https://doi.org/10.2110/palo.2008.
House, M.R., 1978. Devonian ammonoids from the Appalachians and their bearing on international zonation and correlation. Spec. Pap. Palaeontol. 21, 1–70.
Ibrahim, A., 1933. Sporonfermen des Aegirhorizontes des Ruhrreviers. Ph. D. Thesis, Berlinp. 44.
Ishchenko, A.M., 1952. Atlas of microspores and pollen of the Middle Carboniferous Period in the western part of the Donets Basin. Trudy Instituta Geologicheskikh, Akademiya Nauk Ukrainskoy SSR, Transactions of the Institute of Geological Sciences, Academy of Science of the Ukrainian SSR, (Kiev), pp. 1–83.
Jansonius, J., Hills, L.V., Hartkopf-Fröder, C., 2006. *Kraeuselisporites*. Cards 1405 and 5607. In: Genera file of fossil spores - Supplement 14. Special Publication, Dept. Geology and Geophysics. University of Calgary, Calgary, Canada. T2N IN4.
Joachimski, M.M., van Geldern, R., Breisig, S., Day, J., Buggisch, W., 2004. Oxygen isotope evolution of biogenic calcite and apatite during the Middle and Upper Devonian. Int. J. Earth Sci. (Geol. Rundsch.) 93, 542–553.
Johnson, J.G., 1970. Taghanic onlap and the end of north American Devonian provinciality. Geol. Soc. Am. Bull. 81, 2077–2106.
Johnson, J.G., Pendergast, A., 1981. Timing and mode of emplacement of the Roberts Mountains allochthon, Antler orogeny. Geol. Soc. Am. Bull. 92, 648–658.
Johnson, J.G., Sandberg, C.A., 1989. Devonian eustatic events in the western United States and their biostratigraphic responses. In: McMillan, N.J., Embry, A.F., Glass, D.J. (Eds.),

Devonian of the World. Canadian Society of Petroleum Geologists Memoirv. 14, pp. 171–179.
Johnson, J.G., Klapper, G., Sandberg, C.A., 1985. Devonian eustatic fluctuations in Euramerica. Geol. Soc. Am. Bull. 96, 567–587.
Kauffman, M.E., Earll, F.N., 1963. Geology of the Garnet-Bearmouth area, western Montana: Montana Bureau of Mines and Geology. Memoir 39, 40.
Kenrick, P., Fairon-Demaret, M., 1991. *Archaeopteris roemeriana* (Goppert) sensu Stockmans, 1948 from the Upper Famennian of Belgium: Anatomy and leaf polymorphism. Bull. Inst. R. Sci. Nat. Belgiq. Sci. Terre 61, 179–195.
Ketner, K., 2012. An alternative hypothesis for the mid-Paleozoic Antler orogeny in Nevada. USGS Professional Paper 1790, pp. 1–11.
Klapper, G., Johnson, J.G., 1980. Endemism and dispersal of Devonian conodonts. J. Paleontol. 54 (2), 400–455.
Krassilov, V.A., Raskatova, M.G., Istchenko, A.A., 1987. A new archaeopteridalean plant from the Devonian of Pavlovsk, U.S.S.R. Rev. Palaeobot. Palynol. 53, 163–173.
Leanza, A.F., 1968. Acerca del descrubrimiento de ammonoideos devónicos en la República Argentina (*Tornoceras baldisi* n. sp.). Rev. Asoc. Geol. Argent. 23, 326–330.
Leschik, G., 1956. Spores aus den Salzten des Zechsteins von Neuhof (Bei Fulda). Palaeöntogr. Abt. B 100, 125–141.
Limachi, R., Goitia, V.H., Sarmiento, D., Arispe, O., Montecinos, R., Diaz Martínez, E., Dalenz Farjat, A., Liachenco, N., Pérez Leyton, M., Aguilera, E., 1996. Estratigrafía, geoquímica, correlaciones, ambientes sedimentarios y bioestratigrafía del Silúrico-Devónico de Bolivia. 12° Congreso Geológico de Bolivia, Tarija. Memorias 12, 183–197.
Loboziak, S., Melo, J.H.G., 2000. Miospore events from late Early to Late Devonian strata of Western Gondwana. Geobios 33, 399–407.
Loboziak, S., Melo, J.H.G., 2002. Devonian miospore successions of Western Gondwana: update and correlation with Southern Euroamerican miospore zones. Rev. Palaeobot. Palynol. 121, 133–148.
Loboziak, S., Streel, M., 1989. Middle–Upper Devonian miospores from the Ghadamis Basin (Tunisia–Libya): systematics and stratigraphy. Rev. Palaeobot. Palynol. 58, 173–196.
Loboziak, S., Streel, M., Burjack, M.I.A., 1988. Miospores du Dévonien moyen et supérieur du Bassin du Paraná, Brésil: systématique et stratigraphie. Bull. Sci. Géol. 41, 351–377.
Loboziak, S., Streel, M., Weddige, K., 1990. Spores, the *lemurata* and *triangulatus* levels and their faunal indices near the Eifelian/Givetian boundary in the Eifel (F.R.G.). Ann. Soc. Géol. Belgiq. 113 (1991), 1–15.
Loboziak, S., Streel, M., Caputo, M.V., Melo, J.H.G. de, 1992. Middle Devonian to lower Carboniferous miospore stratigraphy in the Central Parnaíba Basin (Brazil). Ann. Soc. Geol. Belg. 115 (1), 215–226.
Loboziak, S., Melo, J.H.G., Matsuda, N.S., Quadros, L.P., 1997. Miospore biostratigraphy of the type Barreirinha Formation (Curuá Group, Upper Devonian) in the Tapajós River area, Amazon Basin, North Brazil. Bull. Centres Rech. Explor. Prod. Elf-Aquitaine 21, 187–205.
Loboziak, S., Melo, J.H.G., Streel, M., 2000. Latest Devonian and Early Carboniferous palynostratigraphy of Northern Brazil and North Africa – a proposed integration of western European and Gondwanan miospore biozonations. Bull. Centres Rech. Explor. Prod. Elf-Aquitaine 22, 241–259.
Lukševičs, E., Lebedev, O.A., Zakharenko, G.V., 2010. Palaeozoogeographical connections of the Devonian vertebrate communities of the Baltica Province. Part I. Eifelian–Givetian. Palaeoworld 19, 94–107.
Malone, D., Welch, J., Foreman, B., Craddock, J., 2017. Detrital Zircon U-Pb geochronology and provenance of the Eocene Willwood Formation, Northern Absaroka Basin, Wyoming. Mt. Geol. 54, 104–124.
Marshall, J.E., 1996a. *Rhabdosporites langii, Geminospora lemurata* and *Contagisporites optivus*: an origin for heterospory within the Progymnosperms. Rev. Palaeobot. Palynol. 93, 159–189.
Marshall, J.E., 1996b. Chapter 29 a. Vegetational history of Devonian spores. In: Jansonius, J., McGregor, D.C. (Eds.), Palynology: Principles and Application. vol. 3. American Association of Stratigraphic Palynologists Foundation, pp. 1133–1141.
Marshall, J.E., 2000. Devonian (Givetian) spores from the Walls Group, Shetland. In: Friend, P.F., Williams, B.P.J. (Eds.), New perspectives on the Old Red Sandstone. Geological Society, London, Special Publications180, pp. 473–483.
Marshall, J.E.A., Allen, K.C., 1982. Devonian miospore assemblages from Fair Isle, Shetland. Palaeontology 25, 277–312.
Marshall, J.E.A., Hemsley, A.R., 2003. A Mid Devonian seed-megaspore from East Greenland and the origin of the seed plants. Palaeontology 46, 647–670.
Marshall, J.E.A., Rogers, D.A., Whiteley, M.J., 1996. Devonian marine incursions into the Orcadian Basin, Scotland. J. Geol. Soc. Lond. 153, 451–466.
Marshall, J.E.A., Miller, M.A., Filatoff, J., Al-Shahab, K., 2007. Two new Middle Devonian megaspores from Saudi Arabia. In: Paris, F., Owens, B., Miller, M.A. (Eds.), Palaeozoic Palynology of the Arabian Plate and Adjacent Areas, Rev. Micropal. 50 (1), pp. 73–79.
Marshall, J.E.A., Brown, J.F., Astin, T.R., 2011. Recognising the Taghanic Crisis in the Devonian terrestrial environment and its implications for understanding land–sea interactions. Palaeogeogr. Palaeoclimatol. Palaeoecol. 304, 165–183.
Marshall, J.E.A., Zhu, H., Wellman, C.H., Berry, C.M., Wang, Y., Xu, H., Breuer, P., 2017. Provincial Devonian spores from South China, Saudi Arabia and Australia. Rev. Micropaleontol. 60, 403–409.
McGregor, D.C., 1960. Devonian spores from Melville Island, Canadian Arctic Archipelago. Palaeontology 3, 26–44.
McGregor, D.C., 1973. Lower and Middle Devonian spores of eastern Gaspé, Canadá I. Systematics. Palaeöntogr. B 142 (1), 77.
McGregor, D.C., 1979. Devonian miospores of North America. Palynology 3, 31–52.
McGregor, D.C., Camfield, M., 1976. Upper Silurian(?) to Middle Devonian spores of the Moose River Basin, Ontario. Geol. Surv. Can. Bull. 263, 1–63.
McGregor, D.C., Camfield, M., 1982. Middle Devonian miospores from the Cape de Bray, Weatherall, and Hecla Bay Formations of northeastern Melville Island, Canadian Arctic. Geol. Surv. Can. Bull. 348, 1–105.
McGregor, D.C., Playford, G., 1992. Canadian and Australian Devonian spores: zonation and correlation. Geol. Surv. Can. Bull. 438, 1–125.
McGregor, D.C., Uyeno, T.T., 1972. Devonian spores and conodonts of Melville and Bathurst Island, District of Franklin. Geol. Surv. Can. Pap. 71, 1–37.
Melo, J.H.G., Loboziak, S., 2003. Devonian - Early Carboniferous miospore biostratigraphy of the Amazon Basin, Northern Brazil. Rev. Palaeobot. Palynol. 124, 131–202.
Meyer-Berthaud, B., Scheckler, S.E., Wendt, J., 1999. *Archaeopteris* is the earliest known modern tree. Nature 398, 700–701. https://doi.org/10.1038/19516.
Meyer-Berthaud, B., Fairon-Demaret, M., Steemans, P., Talent, J., Gerrienne, P., 2003. The plant *Leclercqia* (Lycopisda) in Gondwana: implications for reconstructing Middle Devonian paleogeography. Geol. Mag. 140 (2), 119–130.
Meyer-Berthaud, B., Decombeix, A., Dunstone, R., Gerrienne, P., Momont, N., Young, G., 2016. *Tetraxylopteris* Beck emend. Hammond and Berry (2005), the first aneurophytalean genus recorded in Australia. Rev. Palaeobot. Palynol. 224, 54–65.
Mikesh, D.L., 1965. Correlation of Devonian Strata in Northwestern Wyoming. [Master thesis]University of Iowa.
Mortimer, M.G., Chaloner, W.G., 1967. Devonian megaspores from Wyboston Borehole, Bedfordshire, England. Palaeontology 10 (2), 189–213.
Nance, R.D., Gutiérrez-Alonso, G., Keppie, J.D., Linnemann, U., Murphy, J.B., Quesada, C., Strachan, R.A., Woodcock, N.H., 2012. A brief history of the Rheic Ocean. Geosci. Front. 3, 125–135.
Naumova, S.N., 1939. Spores and pollen of coals of the USSR. Report of the XVII International Geological Congress, Moscow. 1, pp. 355–366.
Naumova, S.N., 1953. Spore- pollen complexes of the Upper Devonian of the Russian Platform and their stratigraphical value. Akad. Nauk S.S.S.R, Geol, Inst. Geol. Ser. 60 (143), 1–204.
Noetinger, S., di Pasquo, M.M., 2011. Devonian palynological assemblages from the San Antonio x-1 borehole, Tarija Basin, northwestern Argentina. Geol. Acta 9 (2), 199–216 (and electronic appendix).
Noetinger, S., 2015. Spore diversity trends in the Middle Devonian of the Chaco-Salteño Plain, northwestern Argentina. Palaeogeogr. Palaeoclimatol. Palaeoecol 417, 151–163.
Noetinger, S., di Pasquo, M., Starck, D., 2018. Middle-Upper Devonian palynofloras from Argentina, systematic and correlation. Rev. Palaeobot. Palynol. 257, 95–116.
Obukhovskaya, T.G., Avkhimovitch, V.I., Streel, M., Loboziak, S., 2000. Miospores from the Frasnian–Famennian Boundary deposits in Eastern Europe (the Pripyat Depression, Belarus and the Timan–Pechora Province, Russia) and comparison with Western Europe (Northern France). Rev. Palaeobot. Palynol. 112, 229–246.
Orlova, O.A., Jurina, A.L., Snigirevsky, S.M., 2016. Late Devonian plant communities of North Russia. Rev. Palaeobot. Palynol. 224, 94–107.
Ottone, E.G., 1996. Devonian palynomorphs from the Los Monos formation, Tarija basin, Argentina. Palynology 20, 105–155.
Owens, B., 1971. Miospores from the Middle and Early Upper Devonian rocks of the Western Queen Elizabeth Islands, Artic Archipelago. Geological Survey of Canada, Pap. 70-38, p. 157.
Palynodata, 2006. https://paleobotany.ru/palynodata/.
Peterson, J.A., 1981. Stratigraphy and sedimentary facies of the Madison limestone and associated rocks in parts of Montana, North Dakota, South Dakota, Wyoming, and Nebraska. USGS Numbered Series 81–642, p. 92.
Playford, G., 1971. Lower Carboniferous spores from the Bonaparte Gulf Basin, Western Australia and Northern Territory. Bureau Miner. Resour. Geol. Geophys. Austr. Bull. 115, 1–105.
Playford, G., 1983. The Devonian miospore genus *Geminospora* Balme 1962: a reappraisal based upon topotypic *G. lemurata* (type species). Mem. Assoc.Austr. Palaeontol. 1, 311–325.
Playford, G., 1985. Palynology of the Australian Lower Carboniferous: a review. International Congress on Stratigraphy and Geology of Carboniferous, Madrid 1983, No. 10, Comptes Rendus. 4, pp. 247–265.
Playford, G., 1991. Australian Lower Carboniferous miospores relevant to extra-Gondwanic correlations: an evaluation. In: Brenckle, P.L., Manger, W.L. (Eds.), Intercontinental correlation and division of the Carboniferous system. Courier Forschungsinstitut Senckenberg 130, pp. 85–125 (Imprinted 1990).
Potonié, R., 1956. Synopsis der Gattungen der *Sporae Dispersae*. I vol. Beihef. Geol. Jah. 23, 1–103.
Potonié, R., Kremp, G.O., 1954. Die Gattungen der Paläozoischen *Sporae dispersae* und ihre Stratigraphie. Beihef. Geol. Jah. 69, 111–194.
Potonié, R., Kremp, G., 1955. Die *Sporae dispersae* des Ruhrkarbons, ihre Morphographie und Stratigraphie mit Ausblicken auf Arten anderer Gebiete und Zeitabschnitte, 1. Palaeöntogr. Abt. B 98, 1–136.
Qie, W., Algeo, T.J., Luo, G., Herrmann, A., 2019. Global events of the late Paleozoic (Early Devonian to Middle Permian): a review. Palaeogeogr. Palaeoclimatol. Palaeoecol. 531, 109259.
Randle, E., Sansom, R.S., 2017. Exploring phylogenetic relationships of Pteraspidiformes heterostracans (stem-gnathostomes) using continuous and discrete characters. J. Syst. Palaeontol. 15 (7), 583–599. https://doi.org/10.1080/14772019.2016.1208293.
Ravn, R.L., Benson, D.G., 1988. Devonian miospores and reworked acritarchs from southeastern Georgia, USA. Palynology 12, 179–200.
Richardson, J.B., 1960. Spores from the Middle Old Red Sandstone of Cromarty, Scotland. Palaeontology 3, 45–63.
Richardson, J.B., 1965. Middle Old Red Sandstone spore assemblages from the Orcadian Basin north-east Scotland. Palaeontology 7 (4), 559–605.
Richardson, J.B., McGregor, D.C., 1986. Silurian and Devonian spore zones of the Old Red Sandstone continent and adjacent regions. Geol. Surv. Can. Bull. 364, 1–79.

Sandberg, C.A., 1961a. Distribution and thickness of Devonian rocks in Williston basin and in central Montana and north-central Wyoming. U.S. Geol. Surv. Bull. 1112-D, 105–127.
Sandberg, C.A., 1961b. Widespread Beartooth Butte Formation of Early Devonian age in Montana and Wyoming and its paleogeographic significance. Am. Assoc. Pet. Geol. Bull. 45 (8), 1301–1309. https://doi.org/10.1306/bc7436e1-16be-11d7-8645000102c1865d.
Sandberg, C.A., 1963. Spirorbal Limestone in the Souris River (?) Formation of Late Devonian age at Cottonwood Canyon, Bighorn Mountains, Wyoming. USGS Professional Paper 475-C, pp. 14–16.
Sandberg, C.A., 1967. Measured sections of Devonian rocks in northern Wyoming. Geological Survey of Wyoming. Wyoming State Geol. Surv. Bull. 52, 1–91.
Sandberg, C.A., McMannis, W.J., 1964. Occurrence and paleogeographic significance of the Maywood Formation of Late Devonian age in the Gallatin range, southwestern Montana. USGS Professional Paper 501-C, pp. 50–54.
Sandberg, C.A., Ziegler, W., Dreesen, R., Butler, J.L., 1988. Late Frasnian mass extinction: Conodont event stratigraphy, global changes, and possible causes. Cour. Forsch. Senckenb. 102, 263–307.
Sandberg, C.A., Morrow, J.R., Warme, J.E., 1997. Late Devonian Alamo Impact Event, global Kellwasser events, and major eustatic events, eastern Great Basin, Nevada and Utah. Brigham Young Univ. Geol. Stud. 42, 129–160.
Sandberg, C.A., Morrow, J.R., Ziegler, W., 2002. Late Devonian sea-level changes, catastrophic events, and mass extinctions. In: Koeberl, C., MacLeod, K.G. (Eds.), Catastrophic Events and Mass Extinctions: Impacts and Beyond. Geological Society of America Special Paper, 356, pp. 473–487 Boulder, Colorado.
Scotese, C.R., 2013. PALEOMAP PaleoAtlas for ArcGIS, Volume 4, Late Paleozoic Paleogeographic, Paleoclimatic and Plate Tectonic Reconstructions. PALEOMAP Project, Evanston, IL. http://www.scotese.com/climate.htm.
Scotese, C.R., Boucot, A.J., McKerrow, W.S., 1999. Gondwanan paleogeography and paleoclimatology, in Gondwana 10: Event Stratigraphy. J. Afr. Earth Sci. 28 (1), 99–114.
Scotese, C.R., Song, H., Mills, B.J.W., van der Meer, D.G., 2021. Phanerozoic paleotemperatures: The earth's changing climate during the last 540 million years. Earth-Science Reviews 215, 103503.
Shen, Z., Monnet, C., Cascales-Miñana, B., Gong, Y., Dong, X., Kroeck, D.M., Servais, T., 2020. Diversity dynamics of Devonian terrestrial palynofloras from China: Regional and global significance. Earth Sci. Rev. 200, 102967.
Staplin, F.L., 1960. Upper Mississippian plant spores from the Golata Formation, Alberta, Canada. Palaeöntogr. Abt. B 107, 1–40.
Staplin, F.L., Jansonius, J., 1964. Elucidation of some Paleozoic densospores. Palaeöntogr. Abt. B 114, 95–117.
Steemans, P., Breuer, P., Petus, E., Prestianni, C., Ville De Goyet, F., Gerienne, P., 2011. Diverse assemblages of Mid Devonian megaspores from Libya. Rev. Palaeobot. Palynol. 165, 154–174.
Steemans, P., Le Hérissé, A., Bozdogan, N., 1996. Ordovician and Silurian cryptospores and miospores from Southeastern Turkey. Review of Palaeobotany and Palynology 93, 35–76.
Steemans, P., Petus, E., Breuer, P., Mauller-Mendlowicz, P., Gerrienne, P., 2012. Palaeozoic innovations in the micro and megafossil plant record: from the earliest plant spores to the earliest seeds. In: Talent, J.A. (Ed.), Earth and Life, International Year of Planet Earth, pp. 437–477.
Stein, W.E., Berry, C.M., Morris, J.L., Hernick, L.V., Mannolini, F., ver Straeten, C., Landing, E., Marshall, J.E.A., Wellman, C.H., Beerling, D.J., Leaket, J.R., 2020. Mid-Devonian *Archaeopteris* roots signal revolutionary change in earliest fossil forests. Curr. Biol. 30, 421–431. https://doi.org/10.1016/j.cub.2019.11.067.
Stock, C.W., 2005. Devonian stromatoporoid originations, extinctions, and paleobiogeography: How they relate to the Frasnian-Famennian extinction. In: Over, D.J., Morrow, J.R., Wignall, P.B. (Eds.), Understanding Late Devonian and Permian-Triassic Biotic and Climatic Events; Towards an Integrated Approach. Developments in Palaeontology & Stratigraphy, 20. Elsevier, Amsterdam, pp. 71–92.
Streel, M., 1964. Une association de spores du Givétien inférieur de la Vesdre, a Goé (Belgique). Ann. Soc. Géol. Bélg. 87, 1–30.
Streel, M., 1967. Association de spores du Dévonien Inférieur Belge et leur signification stratigraphique. Ann. Soc. Geol. Belg. 90 (3), 11–54.
Streel, M., 1972. Dispersed spores associated with *Leclerercqia complexa* Banks, Bonamo, and Grierson from the Late Middle Devonian of eastern new York State (U.S.A). Rev. Palaeobot. Palynol. 14, 205–215.
Streel, M., Loboziak, S., 1987. Nouvelle datation par miospores du Givétien-Frasnien des sédiments non marines du sondage de Booischot (Bassin de Campine, Belgique). Bull. Soc. Belg. Géol. 96, 99–106.
Streel, M., Loboziak, S., 1996. Middle and Upper Devonian miospores. In: Jansonius, J., McGregor, D.C. (Eds.), Palynology: Principles and Applications. vol. 2. American Association of Stratigraphic Palynologists Foundation, pp. 575–587.
Streel, M., Scheckler, S.E., 1990. Miospore lateral distribution in upper Famennian alluvial lagoonal to tidal facies from eastern United States and Belgium. Rev. Palaeobot. Palynol. 64, 315–324.
Streel, M., Higgs, K., Loboziak, S., Riegel, W., Steemans, P., 1987. Spore stratigraphy and correlation with faunas and floras in the type marine Devonian of the Ardenne-Rhenish regions. Rev. Palaeobot. Palynol. 50, 211–229.
Streel, M., Paris, F., Riegel, W., Vanguestaine, M., 1988. Acritarch, chitinozoan and spore stratigraphy from the Middle and Late Devonian of northeast Libya. 111–128. In: El-Arnauti, A., Owens, B., Thusu, B. (Eds.), Subsurface Palynostratigraphy of Northeast Libya. Garyounis University Press Publications, Benghazi, p. 276.
Streel, M., Boulvain, F., Dusar, M., Loboziak, S., Steemans, P., 2021. Updating Frasnian miospore zonation from the Boulonnais (Northern France) and comparison with new data from the Upper Palaeozoic cover on the Brabant Massif (Western Belgium). Geol. Belg. 24 (1–2), 69–84.
Taylor, P.D., Vinn, O., 2006. Convergent morphology in small spiral worm tubes ('*Spirorbis*') and its palaeoenvironmental implications. J. Geol. Soc. Lond. 163, 225–228.
Taylor, T.N., Taylor, E.N., Krings, M., 2009. Paleobotany. The Biology and Evolution of Fossil Plants. Second edition. Elsevier, Amsterdam, p. 1253.
Tel'nova, O.P., 2008. Palynological characterisation of Givetian–Frasnian deposits in the reference borehole section 1, Balneologicheskaya (Southern Timan). Stratigr. Geol. Corr. 16, 143–161.
Tiwari, R.S., 1964. New miospore genera in the Coals of Barakar Stage (Lower Gondwana) of India. The Palaeobotanist 12 (3), 250–259.
Turnau, E., 1996. Miospore stratigraphy of Middle Devonian deposits from Western Pomerania. Rev. Palaeobot. Palynol. 93, 107–125.
Turnau, E., 2014. Floral change during the Taghanic Crisis: Spore data from the Middle Devonian of northern and south-eastern Poland. Rev. Palaeobot. Palynol. 200, 108–121.
Turnau, E., Racki, G., 1999. Givetian palynostratigraphy and palynofacies: new data from the Bodzentyn Syncline (Holy Cross Mountains, central Poland). Rev. Palaeobot. Palynol. 106, 237–271.
van Geldern, R., Joachimski, M.M., Day, J., Jansen, U., Alvarez, F., Yolkin, E.A., Ma, X.-P., 2006. Carbon, oxygen and strontium isotope records of Devonian brachiopod shell calcite. Palaeogeogr. Palaeoclimatol. Palaeoecol. 240, 47–67.
Wan, Z., Algeo, T.J., Gensel, P.G., Scheckler, S.E., Stein, W.E., Cressler III, W.L., Berry, C.M., Xu, H., Rowe, H.D., Sauer, P.E., 2019. Environmental influences on the stable carbon isotopic composition of Devonian and Early Carboniferous land plants. Palaeogeogr. Palaeoclimatol. Palaeoecol. 531, 109100.
Wellman, C.H., 1999. Sporangia containing *Scylaspora* from the Lower Devonian of the Welsh borderland. Palaeontology 42, 67–81.
Wellman, C.H., 2006. Spore assemblages from the Lower Devonian 'Lower Old Red Sandstone' deposits of the Rhynie outlier, Scotland. Trans. R. Soc. Edinb. Earth Sci. 97, 167–211.
Wellman, C.H., Gensel, P.G., Taylor, W.A., 2009. Spore wall ultrastructure of the early Devonian lycopsid *Leclercqia* (Protolepidodendrales) from the Lower Devonian of North America: evidence for a fundamental division in the lycopsids. Am. J. Bot. 96, 1849–1860.
Whiteley, M.J., 1980. Givetian and Frasnian spores from the Key Point Well, Parry Islands, Arctic Canada. Rev. Palaeobot. Palynol. 29, 301–311.
Wood, G.D., Turnau, E., 2001. New Devonian coenobial Chlorococcales (Hydrodictyaceae) from the Holy Cross Mountains and Radom-Lublin region of Poland: Their paleoenvironmental and sequence stratigraphic implications. In: Goodman, D.K., Clarke, R.T. (Eds.), Proceedings of the IX International Palynological Congress, 1996. American Association of Stratigraphic Palynologists Foundation, Houston, Texas, USA, pp. 53–63.
Xu, H., Berry, C.M., Wang, Y., Marshall, J.E.A., 2011. A new species of *Leclercqia* Banks, Bonamo et Grierson (Lycopsida) from the Middle Devonian of North Xinjiang, China, with a possible climbing habit. Int. J. Plant Sci. 172 (6), 836–846.
Xue, J., Huang, P., Wang, D., Xiong, C., Liu, L., Basinger, J.F., 2018. Silurian-Devonian terrestrial revolution in South China: taxonomy, diversity, and character evolution of vascular plants in a palaeogeographically isolated, low-latitude region. Earth Sci. Rev. 92, 92–125.
Young, G.C., 1996. Devonian. In: Young, G.C., Laurie, J.R. (Eds.), An Australian Phanerozoic Timescale. vol. 4. Oxford University Press, Melbourne, pp. 96–109.
Young, G.C., 2003. North Gondwanan mid-Palaeozoic connections with Euramerica and Asia; Devonian vertebrate evidence. Cour. Forsch. Senckenb. 242, 169–185.
Young, G.C., Lu, J., 2020. Asia–Gondwana connections indicated by Devonian fishes from Australia: palaeogeographic considerations. J. Palaeogeogr. 9. https://doi.org/10.1186/s42501-020-00057-x.
Zatoń, M., Vinn, O., Tomescu, A.M.F., 2012. Invasion of freshwater and variable marginal marine habitats by microconchid tubeworms – an evolutionary perspective. Geobios 45, 603–610.
Zatoń, M., Hu, M., di Pasquo, M., Myrow, P.M., 2021. Adaptive function and phylogenetic significance of novel skeletal features of a new Devonian microconchid tubeworm (Tentaculita) from Wyoming, USA. J. Paleontol. https://doi.org/10.1017/jpa.2021.71s.
Ziegler, W., Lane, H.R., 1987. Cycles in conodont evolution from Devonian to mid-Carboniferous. In: Aldridge, R.J. (Ed.), Palaeobiology of Conodonts. British Micropalaeontological Society, pp. 147–163.